8 SCIENTIFIC HIGHLIGHT OF THE MONTH: First Principles Studies of Multiferroic Materials

First Principles Studies of Multiferroic Materials

Silvia Picozzi[1] and Claude Ederer[2]

[1]Consiglio Nazionale delle Ricerche - Istituto Nazionale per la Fisica della Materia (CNR-INFM), CASTI Regional Laboratory, 67100 L'Aquila, Italy

[2]School of Physics, Trinity College, Dublin 2, Ireland

Abstract

Multiferroics, materials where spontaneous long-range magnetic and dipolar orders coexist, represent an attractive class of compounds, which combine rich and fascinating fundamental physics with a technologically appealing potential for applications in the general area of spintronics. *Ab-initio* calculations have significantly contributed to recent progress in this area, by elucidating different mechanisms for multiferroicity and providing essential information on various compounds where these effects are manifestly at play. In particular, here we present examples of density-functional theory investigations for two main classes of materials: a) *proper* multiferroics (where ferroelectricity is driven by hybridization or purely structural effects), with $BiFeO_3$ as prototype material, and b) *improper* multiferroics (where ferroelectricity is driven by correlation effects and is strongly linked to electronic degrees of freedom such as spin, charge, or orbital ordering), with rare-earth manganites as prototypes. As for proper multiferroics, first-principles calculations are shown to provide an accurate qualitative and quantitative description of the physics in $BiFeO_3$, ranging from the prediction of large ferroelectric polarization and weak ferromagnetism, over the effect of epitaxial strain, to the identification of possible scenarios for coupling between ferroelectric and magnetic order. For the class of improper multiferroics, *ab-initio* calculations have shown that, in those cases where spin-ordering breaks inversion symmetry (*i.e.* in antiferromagnetic E-type $HoMnO_3$), the magnetically-induced ferroelectric polarization can be as large as a few $\mu C/cm^2$. The presented examples point the way to several possible avenues for future research: On the technological side, first-principles simulations can contribute to a *rational materials design*, aimed at identifying spintronic materials that exhibit ferromagnetism and ferroelectricity at or above room-temperature. On the fundamental side, *ab-initio* approaches can be used to explore new mechanisms for ferroelectricity by exploiting electronic correlations that are at play in transition metal oxides, and by suggesting ways to maximize the strength of these effects as well as the corresponding ordering temperatures.

1 Introduction to multiferroic materials

Recent years have seen an enormous increase in research activity in the field of multiferroic materials and magneto-electric effects. In December 2007 Science Magazine listed multiferroic

materials as one out of ten "Areas to watch in 2008", the only entry from the Materials Science/Condensed Matter area that was included in this list. First principles calculations using density functional theory (DFT) [1–3] have played an important role in this "Renaissance of Magnetoelectric Multiferroics" [4]. In the present paper we give a brief summary of the current status of research on multiferroic materials and highlight some of the contributions that have been made using first principles electronic structure calculations.

According to the original definition put forward by Hans Schmid [5], multiferroic materials are materials that combine two or more of the primary forms of ferroic order, *i.e.* ferroeleasticity, ferroelectricity, ferromagnetism, and ferrotoroidicity. In practice, most of the recent research has focused on materials that combine some form of magnetic order (ferromagnetic, antiferromagnetic, non-collinear, ...) with ferroelectricity. Therefore, the term *multiferroics* is nowadays often used synonymous with *magnetic ferroelectrics*.

Research on multiferroics (or magnetic ferroelectrics) is also intimately interwoven with research on the *magneto-electric effect*, which is the property that in certain materials a magnetic field induces an electric polarization and, conversely, an electric field induces a magnetization. Traditionally, one distinguishes between linear, quadratic, and higher order magneto-electric effects [6], but more recently the term "magneto-electric effect" is often (mis-)used to describe any form of cross-correlation between magnetic and (di-)electric properties. (For example, when the application of an external magnetic field induces a phase transition between ferroelectric/non-ferroelectric phases.) It is important to point out, though, that not every magnetic ferroelectric exhibits a linear magneto-electric effect (in the original sense) and that not every material that exhibits a linear magneto-electric effect is also simultaneously multiferroic.

Due to the combination of magnetic and dielectric properties, with eventual cross-coupling between these properties, multiferroics have immense potential for technological device applications and at the same time they pose very interesting and rich fundamental physics problems. It is probably this combination of applied and fundamental research that is partly responsible for the strong attraction that these materials have developed in recent years.

Multiferroics form a very diverse class of materials, and there is no unique "theory of multiferroics". Nearly every material has to be studied on its own right, and eventually involves very different physical mechanisms than other multiferroic materials. However, it has proven to be very useful to classify different multiferroics according to the mechanism that drives the ferroelectricity in the corresponding systems. In particular two major classes of multiferroics can be distinguished:

1. Multiferroics, where the ferroelectricity is driven by hybridization and covalency or other purely structural effects.

2. Multiferroics, where the ferroelectricity is driven by some other electronic mechanism, e.g. "correlation" effects.

In the second case, ferroelectricity always arises as a secondary effect that is coupled to some other form of ordering, such as magnetic or charge ordering. Therefore, these systems are often called "improper magnetic ferroelectrics". We note that also in the first class at least one material, hexagonal $YMnO_3$, has been classified as an improper ferroelectric, where the

electric polarization is not the primary order parameter, but instead is coupled to a different non-polar structural instability [7]. In spite of that, and for the purpose of this article, we will call materials belonging to the first category "proper magnetic ferroelectrics" (or "proper multiferroics"), whereas materials in the second category will be called "improper magnetic ferroelectrics" (or "improper multiferroics"). We note that this "zoology" of multiferroics is still work in progress, and that the discovery of new materials might require a further refinement or redefinition of previous classifications.

In this article, we are not attempting to provide a complete review of all first principles work that has been carried out so far. Instead, we discuss some specific examples that illustrate the power of these methods in elucidating the physical origins of the observed properties of known multiferroics, and point out the possibilities in predicting novel effects and designing new materials with optimized properties. Also, we focus only on single-phase (bulk) materials, therefore leaving out all those effects coming from the combination of ferroelectrics and ferromagnets in (artificial) multiferroic heterostructures. Several excellent review articles about general aspects of multiferroic materials and magneto-electric effects have already been published, see for example Refs. [8–13], and much of the early first principles work has also been reviewed in Ref. [14], and more recently in Ref. [15].

The remainder of this article is structured as follows: we start by giving a more detailed discussion of proper magnetic ferroelectrics, and we summarize some of the key developments where first principles studies have made important contributions. We then focus in particular on research related to $BiFeO_3$, which is probably the most studied multiferroic material to date. After that, we give an overview over more recent advancements in the field of improper multiferroics, and discuss some recent work on various manganite systems: orthorhombic E-type $HoMnO_3$ and half-doped $La_{0.5}Ca_{0.5}MnO_3$. We end with some conclusions and perspectives for future research.

Finally, before starting our discussion of proper and improper multiferroics, we want to mention that even though no new calculational techniques have to be developed for the study of these materials, research on multiferroics typically involves a combination of a variety of advanced techniques, most of which have been established only during the last decade (roughly speaking). These techniques include for example beyond-LDA/GGA approaches for the treatment of strongly correlated transition metal oxides, mostly LSDA+U [16,17], methods for the treatment of non-collinear magnetism [18] and spin-orbit coupling [19], the Berry phase approach to calculate electric polarization [20,21] combined with a further analysis using maximally localized Wannier functions [22], and many more.

2 Proper magnetic ferroelectrics

Most of the "early" first principles work on multiferroics was focused on proper magnetic ferroelectrics, in particular on identifying mechanisms for ferroelectricity that are compatible with the simultaneous presence of magnetic order.

In conventional ferroelectrics such as $BaTiO_3$ and $PbTiO_3$, hybridization effects between the filled oxygen p states and the empty transition metal d states are essential for the appearance of the structural instability that causes ferroelectricity [23]. Early first principles work pointed out

that such a mechanism is unfavorable if the transition metal d states are partially filled, which to some extent explains the relative scarcity of magnetic ferroelectrics [24, 25].

The ferroelectricity in multiferroic materials is therefore generally caused by a different mechanism than in prototypical ferroelectric materials such as $BaTiO_3$, $PbTiO_3$, or $KNbO_3$, which all contain transition metal cations with a formal d^0 configuration. As in the case of these conventional ferroelectrics, electronic structure calculations have been crucial in identifying and classifying different mechanisms for ferroelectricity that are also compatible with the simultaneous presence of partially filled d of f states.

Two such mechanisms have emerged from these early studies:

1. Ferroelectricity caused by stereo-chemically active "lone-pair" cations, e.g. Bi^{3+} or Pb^{2+}.
2. "Geometric ferroelectricity", where the structural instability is driven by size effects and other geometrical considerations.

It is well known in chemistry, that cations containing a highly polarizable $5s$ or $6s$ lone pair of valence electrons have a strong tendency to break local inversion symmetry. This can be understood by a mixing between ns and np electron states, which can lower the energy of the cation, but is only allowed if the ionic site is not an inversion center. Alternatively, in a solid this tendency can be understood as cross-gap hybridization between occupied oxygen p and unoccupied np states of the lone-pair cation, similar to the cross-gap hybridization between occupied oxygen p and unoccupied transition metal d states that gives rise to the ferroelectricity in conventional ferroelectrics [26]. In fact, the presence of the lone-pair active Pb^{2+} cation is an important factor for the ferroelectric properties of $PbTiO_3$ (in addition to the presence of the d^0 Ti^{4+} cation) [23]. The lone-pair mechanism was identified as the source of the ferroelectric instability in $BiMnO_3$ [27, 28] and $BiFeO_3$ [29, 30].

In contrast to this, the ferroelectric instability in geometric ferroelectrics does not involve any significant re-hybridization effects. Instead, a structural instability in such systems is generated mainly by size effects and geometric constraints, *i.e.* the space-filling and ionic coordination in the "ideal" high-symmetry structure is not optimal, but can be improved by a small distortion that eventually breaks inversion symmetry. The first material that was identified as geometric ferroelectric is hexagonal $YMnO_3$ [31] (see Fig. 1a). First principles calculations showed that the ferroelectric structure of this material results from an interplay between a polar Γ-point mode and a non-polar Brillouin zone-boundary mode that leads to a unit cell tripling [7, 31]. Furthermore, calculated phonon frequencies together with group theoretical analysis suggests that $YMnO_3$ is an *improper* ferroelectric, where the hexagonal point group of the centrosymmetric high-symmetry structure allows a coupling between the otherwise stable Γ_2^- and the unstable K_3 mode [7].

An example for *proper* geometric ferroelectricity has been found in the series of antiferromagnetic (AFM) fluorides $BaMF_4$, where M can be Mn, Fe, Co, or Ni [32]. The special connectivity of the fluorine octahedra in these systems, which are arranged in quasi-two-dimensional sheets, gives rise to one unstable phonon mode that involves alternating octahedral rotations together with an overall shift of the interjacent Ba cations relative to the other ions (see Fig. 1b). This shift creates an electric dipole moment, and since only one structural mode is involved the

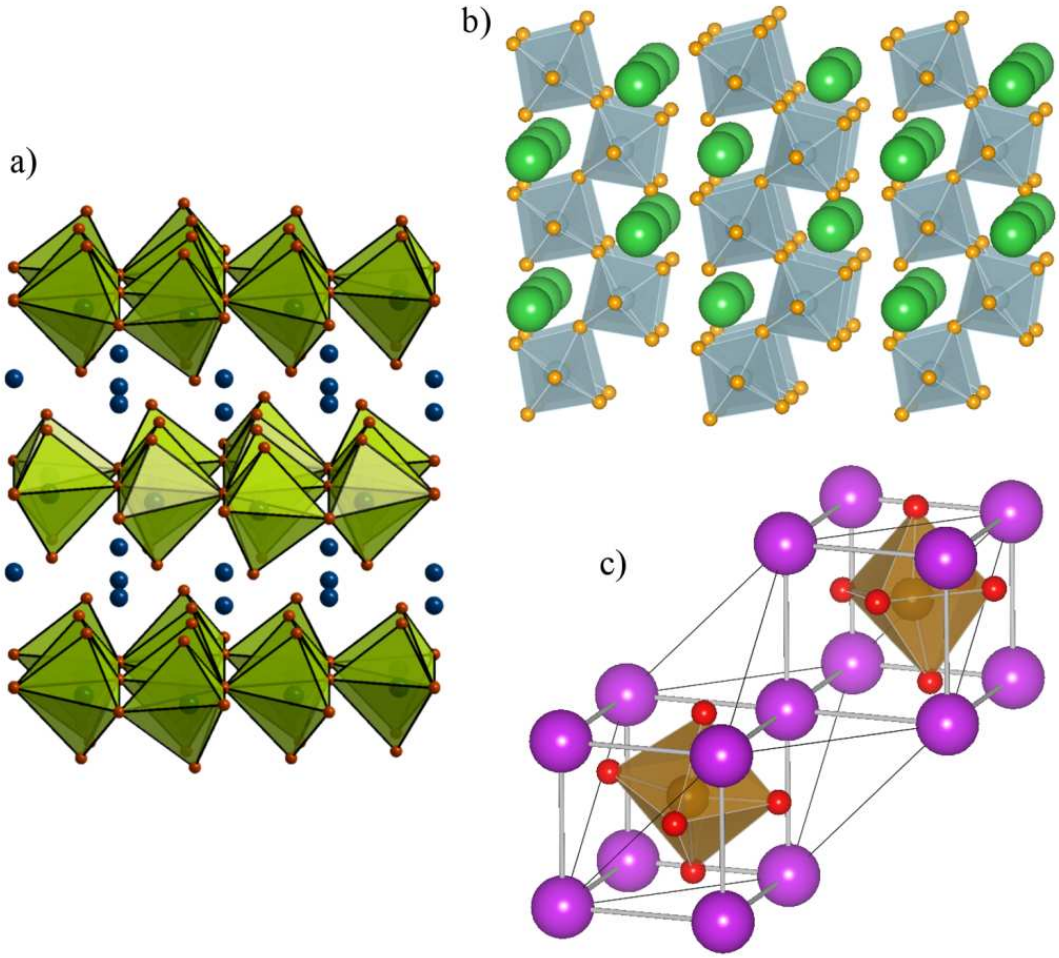

Figure 1: Crystal structures of various magnetic ferroelectrics: a) $YMnO_3$, which has been classified as improper geometric ferroelectric, crystallizes in a layered hexagonal structure, consisting of a two-dimensional arrangement of connected oxygen bi-pyramids surrounding the Mn^{3+} cations that are separated by layers of Y^{3+} cations. b) $BaNiF_4$, a proper geometric ferroelectric, is found in an orthorhombic structure with buckled planes of fluorine octahedra around the Ni^{2+} cations and additional interjacent Ba^{2+} cations. c) $BiFeO_3$, where the ferroelectricity is driven by the stereochemically-active Bi^{3+} cation, exhibits a rhombohedrally distorted perovskite structure, where all ionic sublattices are displaced relative to each other along the polar (111) direction, and the oxygen octahedra are rotated around the same (111) axis, alternately clockwise and counter-clockwise.

corresponding ferroelectricity is classified as "proper". Due to the fact that fluorine systems are generally much more ionic and less covalent than oxides, geometric ferroelectricity can be expected to be the dominant source for ferroelectric instabilities in fluoride compounds.

Very recently, the question of why exactly the standard p-d hybridization mechanism for ferroelectricity is unfavorable for systems with partially filled d shells has been revisited [33, 34]. For perovskite systems, with dominantly cubic crystal field splitting between the t_{2g} and e_g manifolds, it is not fully clear why for example a d^3 configuration with partially filled t_{2g} states, but empty e_g orbitals, cannot give rise to a favorable cross-gap hybridization between filled oxygen p and empty transition metal e_g states. It was suggested that the Hund's coupling between t_{2g} and e_g states will disfavor such hybridization [11]. This was supported by LDA+U calculations for $CaMnO_3$, where the Hund's coupling was effectively "turned off", which indeed resulted in a tendency for off-centering of the Mn^{4+} cation. In addition, recent first principles calculations for $CaMnO_3$, $SrMnO_3$, and $BaMnO_3$ in the perovskite structure show that these systems can develop a ferroelectric instability, but that this ferroelectric instability competes with a non-polar "antiferrodistortive" instability, and that the relative strength of these two instabilities depends strongly on the unit cell volume [33, 34]. For larger volumes (*i.e.* $BaMnO_3$) the ferroelectric instability becomes dominant. Thus, even though $BaMnO_3$ is not stable in the cubic (or in the orthorhombically distorted) perovskite structure (it crystallizes in a hexagonal structure), this opens up the possibility to stabilize the corresponding ferroelectric phase by using epitaxial constraints, *i.e.* using thin film growth techniques.

Apart from these investigations into possible mechanisms for ferroelectricity that are compatible with the simultaneous presence of magnetic order, first principles calculations have also been used to rationalize experimental observations, investigate possible mechanisms for coupling between the electric polarization and the magnetic order, and to design new multiferroic and magnetoelectric materials. In the following we will highlight some of these calculations, in particular the work related to one of the most prominent multiferroic materials: bismuth ferrite.

2.1 First principles calculations for $BiFeO_3$ and related work

$BiFeO_3$ (BFO) is one of the most studied (probably *the* most studied) multiferroic material. BFO is known to be multiferroic (or more precisely: AFM and ferroelectric) already since the early 1960s [35]. However, for a long time it was not considered as a very promising material for applications, since the electric polarization was believed to be rather small [36] and the AFM order does not lead to a net magnetization [37, 38].

This has changed drastically, following a publication in Science in 2003 (Ref. [39]), which to great extent has triggered the intensive experimental and theoretical/computational research on BFO during the last 5–6 years. In this study, a large spontaneous electric polarization in combination with a substantial magnetization was observed above room temperature in thin films of BFO grown epitaxially on $SrTiO_3$ substrates. The presence of both magnetism and ferroelectricity above room temperature, together with potential coupling between the two order parameters, makes BFO the prime candidate for device applications based on multiferroic materials.

Whereas the large electric polarization was later confirmed independently, and explained by first

principles calculations, the origin of the strong magnetization reported in [39] is still unclear and, to the best of our knowledge, it has never been reproduced in an independent study. It is generally assumed that the magnetization reported in Ref. [39] is related to extrinsic effects such as defects or small amounts of impurity phases.

The large electric polarization, which appeared to be at odds with bulk single crystal measurements from 1970 [36], was originally assumed to be due to epitaxial strain, which results from the lattice constant mismatch between BFO and the substrate material $SrTiO_3$. It is known that epitaxial strain can have drastic effects on the properties of thin film ferroelectrics. For example, it can lead to a substantial enhancement of electric polarization and can even induce ferroelectricity at room temperature in otherwise non-ferroelectric $SrTiO_3$ [40, 41].

In the following we illustrate how first principles calculations have been instrumental in clarifying the origin of both polarization and magnetization in thin film BFO, by showing that the large electric polarization found in the thin films is in fact intrinsic to unstrained bulk BFO and that, in contrast to many other ferroelectrics, epitaxial strain has only a minor effect in this material.

2.1.1 Electric polarization of bulk BFO and the effect of epitaxial strain

According to the so-called "Modern theory of polarization", the electric polarization of a bulk periodic system is defined via the Berry phase of the corresponding wavefunctions [20, 21]. Since this geometrical phase is only well defined modulo 2π, the polarization is only well-defined modulo so-called "polarization quanta", given by $\Delta\vec{P}_0^{(i)} = \frac{fe}{\Omega}\vec{a}_i$, where e is the electronic charge, $\vec{a}_i$ a primitive lattice vector ($i = 1, 2, 3$), Ω the unit cell volume, and f is a spin degeneracy factor ($f = 2$ for a non-spinpolarized system, $f = 1$ for a spin-polarized system). If the expression for the polarization is recast as a sum over "Wannier centers" [20], a translation of one of the occupied Wannier states from one unit cell to the next corresponds to a change in polarization by exactly one "quantum". The multivaluedness thus reflects the arbitrary choice of basis vectors when describing an infinite periodic structure.

In spite of this multivaluedness of the bare polarization for a specific atomic configuration, differences in polarization are well defined quantities, provided the corresponding configurations can be transformed into each other in a continuous way and the system remains insulating along the entire "transformation path" [21].

In particular, the spontaneous polarization of a ferroelectric material is defined as half the difference in polarization between two oppositely polarized states, or equivalently, as the difference in polarization between the ferroelectric structure and a suitable centrosymmetric reference configuration. In order to calculate the spontaneous polarization one therefore has to perform a series of calculations for different configuration between the ferroelectric state and the centrosymmetric reference structure. If the change in polarization between two such configurations is much smaller than the polarization quantum, then the corresponding difference can be clearly identified and the full change in polarization along the transformation path, *i.e.* the spontaneous polarization, can be determined.

The application of this procedure to calculate the spontaneous polarization of BFO is complicated by the following two features: *i)* the polarization quantum for a spin-polarized system is

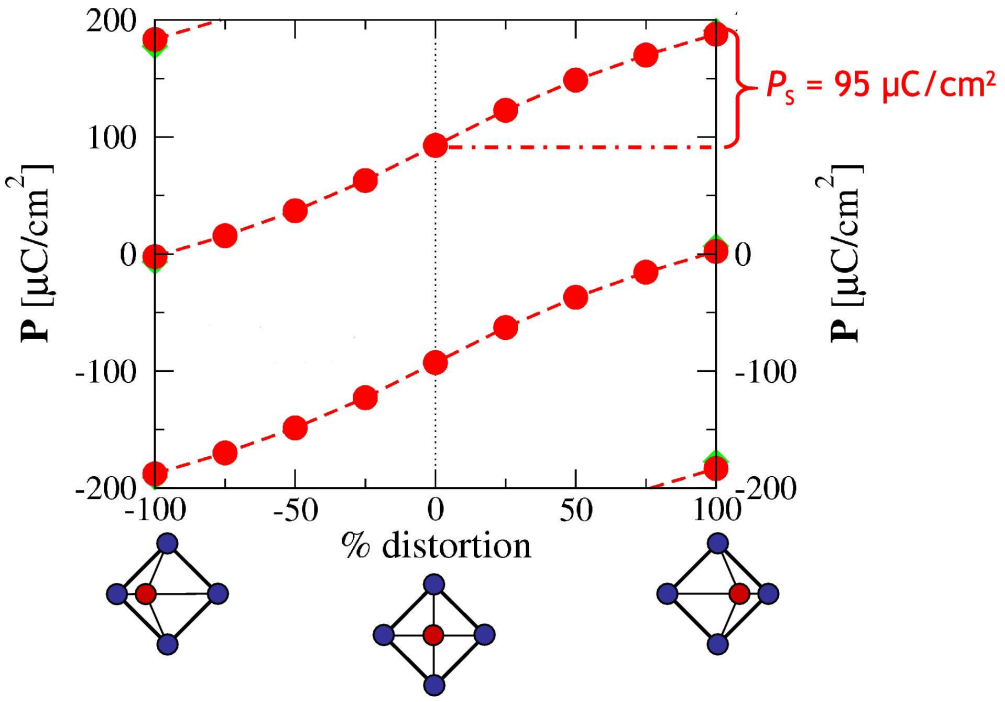

Figure 2: Evolution of the polarization P along the transformation path from a negatively polarized state (-100 % distortion), through a centrosymmetric reference configuration (0 % distortion), to a positively polarized state ($+100$ % distortion). Red circles correspond to the LSDA+U calculation with $U_{\rm eff} = 2$ eV, green diamonds indicate the LSDA result for the fully polarized states. Different values of P for fixed amount of distortion are separated by the polarization quantum $\Delta P_0^{(111)} = 186$ μC/cm^2. The spontaneous polarization P_s is given by the difference in polarization between the fully distorted and the undistorted configuration for an arbitrary branch of the bare polarization. Note: the systematic sketches at the bottom do not correspond to the actual crystal structure of BFO.

only half that for a similar nonmagnetic system, and *ii)* due to the underestimation of the local spin splitting for Mott-Hubbard insulators within the standard local spin-density approximation (LSDA), BFO becomes metallic for the less distorted reference configurations within LSDA.

These problems have been overcome in Ref. [29] by using the LSDA+U method [16, 17] to calculate the electronic structure of BFO in various configurations along the transformation path from the fully distorted $R3c$ structure to the centrosymmetric cubic perovskite ($Pm\bar{3}m$) structure. Within the LSDA+U method the local d-d exchange splitting is enhanced by the Hubbard U and BFO stays insulating even in the undistorted cubic perovskite structure (for U values $U_{\rm eff} = U - J = 2$–4 eV [29]).

Figure 2 shows the evolution of the electric polarization with varying degree of distortion between two oppositely polarized states calculated for $U_{\rm eff} = 2$ eV. The LSDA results are included for ± 100 % distortion. The fact that the corresponding symbols (green diamonds) can barely be recognized behind the red circles that indicate the LSDA+U results shows that the value of the bare polarization is rather insensitive to the exact value of $U_{\rm eff}$. It can be seen that different values of P corresponding to the same amount of distortion are separated by the polarization

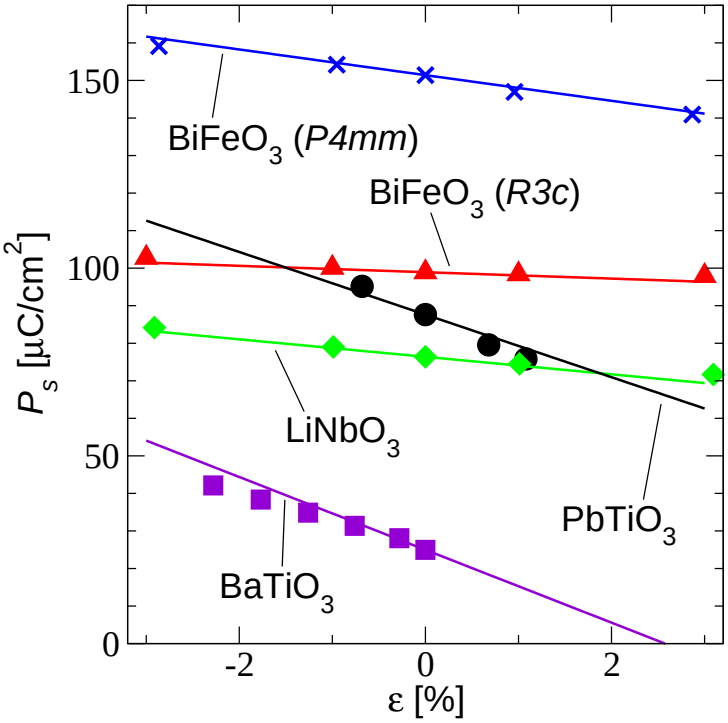

Figure 3: Dependence of the spontaneous polarization P_s on epitaxial strain ϵ for BFO in two different structural modifications and some other (non-magnetic) ferroelectrics. Symbols correspond to results from first principles calculations for strained unit cells (data for $BaTiO_3$/$PbTiO_3$ is taken from [43]/ [44]), lines are obtained from the calculated bulk linear response functions (see [45]). Note that the epitaxial constraint for all systems is applied in the plane perpendicular to the polarization, *i.e.* (001) for $BaTiO_3$, $PbTiO_3$, and $P4mm$-$BiFeO_3$, and (111) for $LiNbO_3$ and $R3c$-$BiFeO_3$.

quantum along (111), $\Delta P_0^{(111)} = \frac{e}{\Omega}(\vec{a}_1 + \vec{a}_2 + \vec{a}_3)$, where $\vec{a}_{1,2,3}$ are the primitive lattice vectors of the rhombohedral $R3c$ structure. As indicated, the spontaneous polarization P_s can be obtained as the difference between the fully distorted and the undistorted configuration for an arbitrary "branch" of the bare polarization.

From these calculation a spontaneous polarization of bulk BFO of $\sim$ 95 μC/cm^2 has been obtained. This is an order of magnitude larger than what was previously believed to be the case, based on the measurements in Ref. [36], and even exceeds the polarization of typical prototype ferroelectrics such as $BaTiO_3$, $PbTiO_3$, or $PbZr_{0.5}Ti_{0.5}O_3$ (PZT). Variation of U_{eff} within reasonable limits changes the calculated value for the electric polarization by only $\sim \pm 5$ μC/cm^2, *i.e.* the large value of the polarization is rather independent from the precise value of the Hubbard parameter. This is consistent with the assumption that the transition metal d states do not play an active role for the ferroelectric instability in BFO. The calculated large spontaneous polarization for bulk BFO is also consistent with the large ionic displacements in the experimentally observed $R3c$ structure of BFO (see Fig. 1c), compared to an appropriate centrosymmetric reference configuration. Recently, the large polarization of $\sim$ 100 μC/cm^2 along (111) for bulk BFO has also been confirmed experimentally by new measurements on high-quality single crystals [42].

Effects of epitaxial strain can be assessed from first principles by performing bulk calculations for a strained unit cell, where the lattice constant within a certain lattice plane (corresponding to the orientation of the substrate surface) is constrained, whereas the lattice constant in the perpendicular direction as well as all internal structural parameters are allowed to relax. Such calculations have been performed for BFO corresponding to a (111) orientation of the substrate [46]. In this case the $R3c$ symmetry of the bulk structure is conserved and the epitaxial constraint is applied in the lattice plane perpendicular to the polarization direction. It was found that the sensitivity of the electric polarization to strain is surprisingly weak in BFO, much weaker than in other well-known ferroelectrics [46] (see Fig. 3). A systematic comparison of the strain dependence in various ferroelectrics, including BFO in both the $R3c$ and a hypothetical tetragonal phase with $P4mm$ symmetry, has been performed in Ref. [45] (see Fig. 3). It was shown that the effect of epitaxial strain for all investigated systems can be understood in terms of the usual bulk linear response functions and that both strong and weak strain dependence can occur.

Systematic calculations corresponding to a (001) orientation of the substrate, the one that is most often used experimentally, have not been performed so far. Since the epitaxial constraint in this case breaks the rhombohedral symmetry of the bulk structure, the corresponding strained unit cell has a lower symmetry with more free parameters than in the (111)-strained case. Nevertheless, the effect of such a monoclinic strain on the ferroelectric polarization in BFO has been investigated by performing calculations for a set of lattice parameters derived from representative experimental data. Due to the lower symmetry, the polarization in this case is slightly rotated away from the (111) direction, but the overall magnitude remains nearly unchanged compared to the unstrained case. From this it was concluded that the polarization in BFO is generally rather insensitive to epitaxial strain, and that the large polarization measured in thin films is basically the same as in the corresponding bulk system. Indeed, the polarization of ~ 60 μC/cm^2 reported in Ref. [39] for a (001) oriented thin film agrees well with the corresponding projection of the calculated bulk value (which is oriented along the (111) direction), and polarization measurements for BFO films with different substrate orientations ((001), (101), and (111)) can all be understood by assuming that the polarization vector in all cases points essentially along (111) and has approximately the same length [47]. More recently, systematic experimental investigations of the strain effect in epitaxial BFO films have been undertaken by comparing results of BFO films with different thicknesses, which have confirmed the predicted weak strain dependence of the polarization in BFO [48]

Finally, it should be noted that Ref. [39] also contains results of first principles calculations for the electric polarization of two structural variants of BFO: the rhombohedral bulk structure with $R3c$ space group, and a hypothetical tetragonal structure with $P4mm$ symmetry, based on the lattice parameters found in the thin film samples. At that time it was assumed that such a tetragonal phase is stabilized in epitaxial thin films and that the difference in polarization observed in thin films compared to bulk BFO was due to a large difference in polarization between the two different structural modifications. However, the DFT results presented in Ref. [39] were not conclusive, since only the bare polarization for the two different structures was reported and not the spontaneous polarization that is measured in the corresponding "current-voltage" switching experiments.

In fact, it is indeed possible that a different phase is stabilized in thin films, which can then lead to more significant changes of ferroelectric and magnetic properties compared to bulk BFO. However, it is important to distinguish between the simple case of a somewhat distorted version of the rhombohedral bulk structure and a truly different phase, which would for example be characterized by a different oxygen octahedra tilt pattern or a different number of formula units contained in the crystallographic unit cell.

Calculations presented in Ref. [45] (see also [49]) show that if BFO is constrained to tetragonal $P4mm$ symmetry (with no octahedral tilts and only one formula unit per unit cell) it develops a "super-tetragonality" with c/a ratio of 1.27 and a giant electric polarization of $P_s \approx 150\ \mu\mathrm{C/cm}^2$. A polarization of this magnitude has indeed been found in some highly strained films with c/a ratios between 1.2–1.3 [49, 50], whereas many other experimental reports of "tetragonal" BFO films with smaller c/a ratio also exist. These reports should be regarded with some caution, since the structural characterization of thin films is usually restricted to the measurement of lattice constants and of angles between certain crystallographic directions. A full characterization of ionic distortions (including octahedral tilt patterns etc.) is generally not possible for thin films, and first principles calculations can therefore play an important role in clarifying open questions about the exact thin film structure of BFO. In principle, if one tries to epitaxially match the rhombohedral bulk structure of BFO on a square lattice substrate plane, one can expect to obtain a monoclinically distorted version of the BFO bulk structure. However, since the rhombohedral angle in bulk BFO is very close to 60°, the value that corresponds to an underlying cubic lattice, the monoclinic distortion can be rather small, and the thin films might appear essentially tetragonal.

2.1.2 Weak ferromagnetism in thin film BFO and coupling between the various order parameters

In addition to these structural studies, DFT calculations have also been used to investigate the magnetic properties of BFO, in particular the possible origin for the significant magnetization reported in Ref. [39]. Bulk BFO is known to exhibit "G-type" AFM ordering [37], *i.e.* the magnetic moment of each Fe cation is antiparallel to that of its nearest neighbors. Superimposed to this G-type magnetic order a long-period cycloidal modulation is observed, where the AFM order parameter $\vec{L} = \vec{M}_1 - \vec{M}_2$, defined as the difference between the two sublattice magnetizations $\vec{M}_{1,2}$, rotates within the (110) plane with a wavelength of ~ 620 Å [38].

Calculations for bulk BFO show a very strong and dominant AFM nearest neighbor interaction [51], in agreement with the observed G-type magnetic order and the rather high Néel temperature of ~ 600 K. In addition, the magnetocrystalline anisotropy has been calculated, and a preferred orientation of the Fe magnetic moments perpendicular to the polar [111] direction has been found [52]. Within the (111) plane a 12-fold degeneracy remains, leading to an effective "easy-plane" geometry for the magnetic moments. For an orientation of the AFM order parameter $\vec{L}$ within this (111) plane, *weak ferromagnetism* is symmetry-allowed, *i.e.* a small canting of the two AFM sublattice magnetizations can occur, which results in a net magnetization [53]. Indeed, if spin-orbit coupling is included in the calculation (while the cycloidal modulation is neglected), a small canting of the magnetic moments is obtained [52]. The magnitude of the resulting

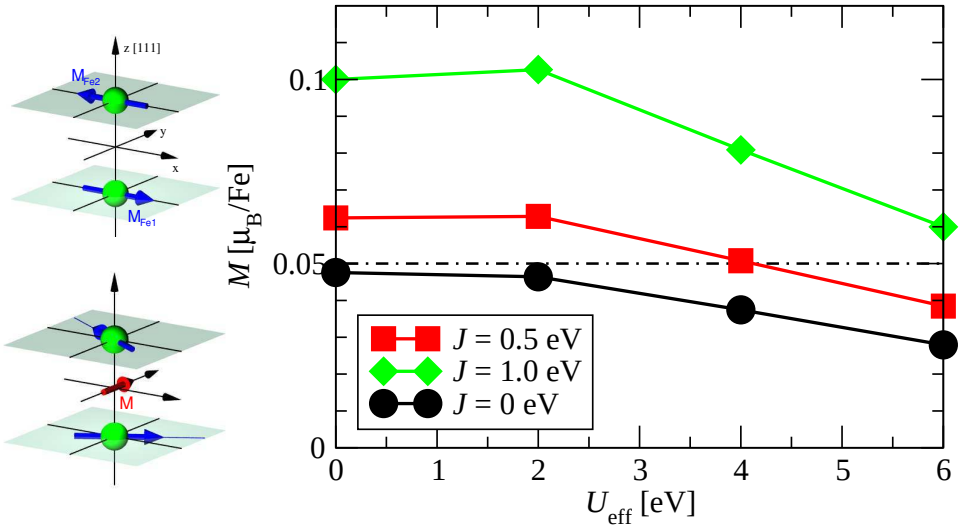

Figure 4: Dependence of the weak magnetization in BFO on the LSDA+U parameters $U_{\text{eff}} = U - J$ and J. The dash-dotted line represents the reported value of 0.05 μ_B/Fe. The sketches on the left side illustrate how the canting of the two AFM sublattice magnetizations, represented by the magnetic moments M_{Fe1} and M_{Fe2} of the two Fe cations in the primitive unit cell, gives rise to the net magnetization M.

magnetization depends on the choice of the Hubbard U and the Hund's rule parameter J, but for reasonable values of $U_{\text{eff}} = U - J$ the magnetization is around 0.05 μ_B/Fe cation (see Fig. 4). This value of the magnetization agrees quite well with various thin film measurements [54–56], but is significantly smaller than what was originally reported in Ref. [39]. It has to be pointed out that no magnetization is observed in bulk BFO, where the presence of the cycloidal modulation effectively cancels any net magnetic moment. If the cycloidal modulation is suppressed, either by applying a strong magnetic field [57] or by chemical substitution [58] a small magnetization appears, with comparable magnitude to the computational result. It is generally assumed that the cycloidal rotation of the AFM order parameter is also suppressed in thin films, likely due to enhanced anisotropy, and that the small magnetization observed in the thin films is due to weak ferromagnetism. This is supported by a neutron diffraction study on BFO films, which could not find the satellite peaks associated with the cycloidal modulation [56].

Furthermore, first principles studies addressing the effect of epitaxial strain and the presence of oxygen vacancies did not find a significant increase in magnetization [46], and it is therefore likely that the large magnetization reported in [39] is due to other defects or small amounts of impurity phases.

The appearance of weak ferromagnetism in thin films of BFO leads to the question of whether this small magnetization is coupled to the electric polarization, *i.e.* whether it can be manipulated by applying external electric fields. Indeed, the absence of an inversion center located at the midpoint between two interacting magnetic moments is crucial to produce a non-vanishing *Dzyaloshinskii-Moriya (DM) interaction*, which has been identified as the microscopic mechanism responsible for the magnetic moment canting in weak ferromagnets [59]. Thus, inversion symmetry breaking can cause both weak ferromagnetism and ferroelectricity, suggesting possible cross-correlations between these two properties. First principles calculations have been used to

explore this possibility for magnetization-polarization coupling in BFO [52] and in $BaNiF_4$ [60]. It was found that in BFO the DM interaction is caused by a non-polar antiferrodistortive mode, not by the polar distortion, and therefore the weak ferromagnetism in BFO is not controlled by the spontaneous polarization and cannot be switched using an electric field [52]. In contrast, in $BaNiF_4$, it is indeed the polar distortion that creates a DM interaction, but the symmetry is such that no net magnetization results. Instead, a secondary (weak) AFM order parameter is induced in addition to the distinctly different primary AFM order [60]. Only recently, a material has been suggested, based on a combination of first principles calculations and symmetry considerations, that fulfills all requirements for "ferroelectrically-induced weak ferromagnetism" [61]. The corresponding material, $R3c$ structured $FeTiO_3$, is closely related to BFO in that it has the same overall structural symmetry, but with the magnetic Fe cations located on the perovskite A site instead of the perovskite B site as in BFO. It is this difference in the local site symmetry of the magnetic cation, that is crucial for the coupling between the spontaneous polarization and the weak magnetization [61, 62]. Experimental work is currently underway to validate this theoretical prediction.

2.1.3 Designing new multiferroics and new functionalities

The prediction of $FeTiO_3$ as a possible candidate for electric field switchable weak ferromagnetism, is one example for attempts to design new materials with novel or more favorable magneto-electric properties based on first principles electronic structure calculations.

Another example is the design of a material that allows for magneto-electric phase control [63]. Calculations for the rare-earth magnet $EuTiO_3$ showed that this material exhibits a soft infrared-active, *i.e.* polar, phonon mode that becomes unstable if the material is epitaxially strained. In addition, due to strong spin-phonon coupling in this material, the instability is more pronounced for ferromagnetic ordering of the Eu spins than for the case of an AFM arrangement. Since the ground state magnetic structure for the lower strain region is AFM, it was suggested that a phase transition from a non-polar AFM phase into a ferroelectric-ferromagnetic phase can be induced by applying a strong magnetic field, if the material can be prepared in thin films with a compressive epitaxial strain of around 1 % [63].

In addition, attempts have been made to design materials that combine strong ferroelectric polarization with a large magnetization above room temperature. If such a material would also exhibit pronounced coupling effects between polarization and magnetization, which ideally would allow to switch the polarization via a magnetic field or vice versa, then this would probably create a similar excitement as finding a room temperature superconductor. Unfortunately, at the moment no multiferroic that exhibits all these properties is known (similarly, no room temperature superconductor is known at present).

A suggestion for a material combining large polarization and large magnetization has been made in Ref. [64]. First principles calculations predict, that if half of the Fe^{3+} cations in BFO are replaced by Cr^{3+} cations in a checkerboard-like ordered arrangement, then the resulting material Bi_2FeCrO_6 is stable in a rhombohedral structure similar to BFO with a spontaneous ferroelectric polarization of around 80 $\mu C/cm^2$ and a magnetization of 2 μ_B per formula unit. The magnetization in this case results from a ferri-magnetic arrangement, where the magnetic

moments of the Cr cations are antiparallel to those of the Fe cations. A subsequent study of the strength of the magnetic coupling in the series of compounds $BiFeO_3$-Bi_2FeCrO_6-$BiCrO_3$ has found that the Néel-temperature in Bi_2FeCrO_6 is unlikely to be above room temperature [51], but nevertheless several attempts have been made to synthesize the corresponding material [65–67]. The synthetic challenge here, is to achieve the required checkerboard-type ordering of Fe and Cr cations on the B sites of the underlying perovskite structure, which might be possible by utilizing layer-by-layer growth on a (111)-oriented substrate.

2.2 Perspectives for future studies of proper multiferroics

The examples discussed so far show that first principles calculations have proven not only to be useful for rationalizing experimental observations and identifying different mechanisms for ferroelectricity that can be found in multiferroic materials, but also to facilitate quantitative predictions of new materials and novel effects in proper magnetic ferroelectrics. Future applications of *ab initio* methods in the design of new materials and in calculating the expected properties of these materials are therefore expected to continue to have a significant impact on the overall progress of this field.

In particular, a material with large magnetization and large polarization above room temperature is still elusive. From the current point of view there is no fundamental reason why such a material should not exist, and creative ideas on how to circumvent the limitations and restrictions of materials chemistry that have been encountered so far are still highly desirable.

Another area where DFT will undoubtedly have (and already has) a substantial impact, is the study of artificial heterostructures consisting of a combination of magnetic and ferroelectric materials [13]. Examples of computational work in that direction that have already appeared include the study of artificial tri-layered superlattices of different magnetic and nonmagnetic oxides [68] and the investigation of polarization effects at the interface between a ferromagnetic metal and a ferroelectric insulator [69].

3 Improper Multiferroics

In the beginning of this section, we will focus on the origin of ferroelectricity in the so-called "Improper multiferroics" (IMF), outlining a few differences with respect to the more conventional "proper" multiferroics discussed so far.

As pointed out in the previous sections, in displacive ferroelectric materials (such as prototypical perovskite-like $BaTiO_3$ or multiferroic $BiFeO_3$), due to strong covalency effects, the relative displacement of the anionic sublattice with respect to the cationic sublattice gives rise to a spontaneous and switchable polarization, which is the (primary) order parameter in the ferroelectric transition. On the other hand, in IMF, the primary order parameter of the phase transition is related to electronic (*i.e.* spin, charge, or orbital) degrees of freedom [12]. The important thing is that the resulting electronic order lacks inversion symmetry (IS), therefore opening the way to ferroelectricity. Therefore, polarization occurs as a by-product of the electronic phase transition and can be described as a "secondary" order parameter. As a consequence, *i*) even

the state with ions pinned in centrosymmetric positions can show a finite (purely electronic) polarization; *ii*) the ions can "react" to the non-centrosymmetric charge-redistribution by displacing, so as to give a (more traditional) ionic contribution to the total polarization. In order to push ahead with the comparison between proper and improper multiferroics, one can say that ferroelectricity in IMF is driven by "correlation" effects (as related to spin or charge arrangements), at variance with the previously mentioned case of standard ferroelectrics where it is mostly driven by covalency. In IMF where polarization is magnetically-induced, it is reasonable to expect a strong coupling between magnetic and ferroelectric properties, since the two dipolar and magnetic orderings share the same origin and occur at the same temperature.

In Fig. 5 we schematically classify IMF on the basis of the different mechanisms to induce ferroelectricity that have been proposed so far. We would like to point out that what we present in the following is a non-exhaustive list of the IMF materials and related mechanisms. In fact, IMF represent a quickly evolving field: new materials and/or novel mechanisms are proposed on a monthly or even weekly basis. With no doubt, we therefore expect in the near future this classification to become richer in compounds and to expand as far as mechanisms are concerned.

In Fig. 5 IMF are divided in two main classes: those where ferroelectricity is driven by spin-order (*i.e.* where the "magnetic" arrangement breaks IS) and those where it is driven by charge-order (*i.e.* where the charge-disproportionation leads to a non-centrosymmetric arrangement). In turn, the magnetically-induced ferroelectricity can occur in two different ways: *i*) the first and most studied case where a non-collinear spin-spiral occurs and the IS-breaking arises due to a spin-orbit related mechanism in the DM-like antisymmetric exchange term [70–72]; *ii*) the case of (mostly collinear) AFM spins where the IS-breaking occurs in the Heisenberg-like symmetric exchange-term [73, 74].

Along with the classification of IMF, we show in Fig. 5 a few links to IMF materials for which *ab-initio* studies have been reported in the literature.

Chronologically, the recent interests towards IMF were boosted by the discovery of ferroelectricity in $TbMnO_3$ and of the control of the polarization direction achieved via an applied magnetic field [87]. However, the *ab-initio* simulations for $TbMnO_3$ came much later [75, 76], due to the complexity in the related simulations: advanced capabilities (such as non-collinear magnetism and spin-orbit coupling) are needed to reproduce the observed tiny effects, which implicitly requires a high precision in terms of numerical parameters in the calculations. In the *ab-initio* field, the first IMF to be studied were collinear antiferromagnets, such as $TbMn_2O_5$ [81] and $HoMnO_3$ [74]. Since the latter will be described in detail in Sec. 3.1.1, we will now briefly discuss the first one. The class of manganites often labeled as "1-2-5" from the stoichiometry of rare-earth, transition metal, and oxygen, respectively, is an actively studied set of IMF. Despite some non-collinearity and non-commensurability effects, most of the mechanisms behind multiferroicity can be described through simulations with non-centrosymmetric collinear spin arrangement using a relatively small supercell. The suggested polarization was of the order of 1 $\mu C/cm^2$ and the polarization was reversed by changing the spin-orientation in the unit cell, providing evidence for the magnetic origin of ferroelectricity in $TbMn_2O_5$. Within the same class of materials, $HoMn_2O_5$ was studied in Ref. [82]: the main and new result of that work was that the ionic and electronic contributions were strongly dependent on the value of the Hubbard

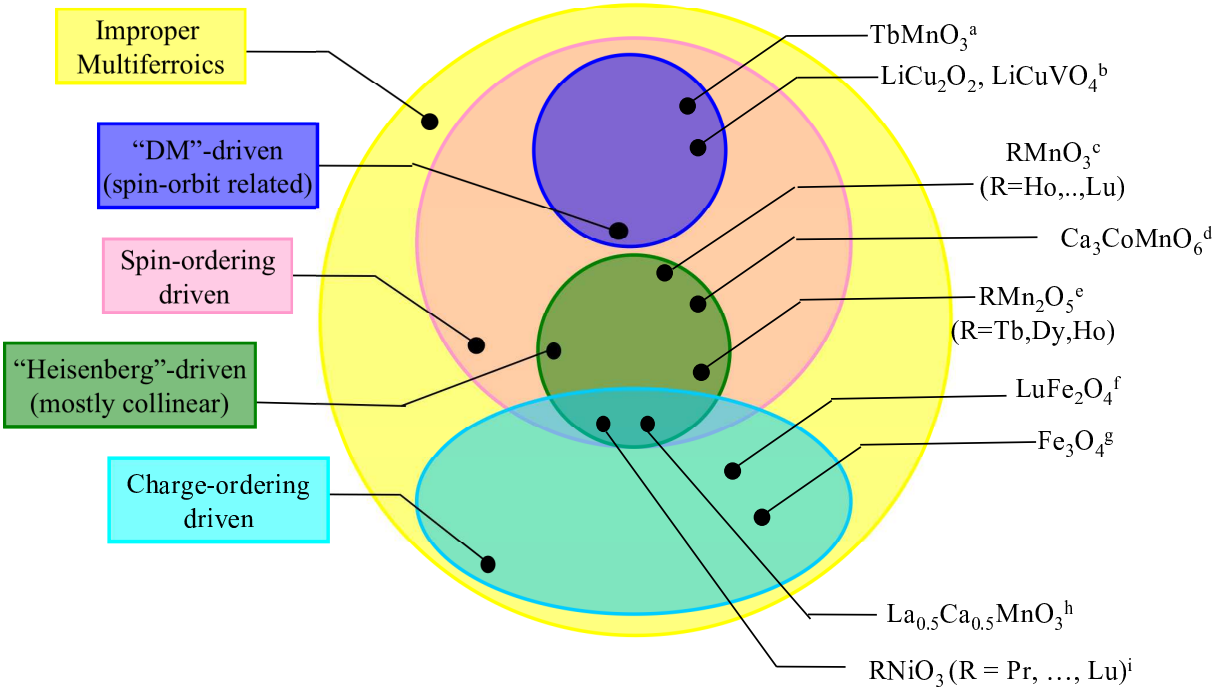

Figure 5: Schematic classification of IMF, in terms of different mechanisms (left side) and compounds (right side). The (non comprehensive) list includes a few materials which were studied by first-principles (see related references: a) Ref. [75, 76], b) Ref. [77], c) Ref. [74, 78], d) Ref. [79, 80], e) Ref. [81, 82], f) Ref. [83], g) Ref. [84], h) Ref. [85], i) Ref. [86]).

U parameter used in a LSDA+U approach, pointing to the important role of correlation effects in 1-2-5 manganites.

Within the spin-spiral class of IMF, Li-Copper-based oxides were the first compounds to be studied from first-principles [77]: upon switching-on spin-orbit coupling, the calculated polarization was rather small (of the order of tens or hundreds of μC/cm^2, depending on whether ionic relaxations were included or not in the simulations). Shortly later, the prototypical case of $TbMnO_3$ was published in two important papers (one following the other in Phys. Rev. Lett.), Refs. [75, 76]. It was shown that the purely electronic contribution (*i.e.* evaluated by switching on spin-orbit but keeping the ions frozen into their paramagnetic centrosymmetric configuration) was much smaller than the ionic contribution (*i.e.* evaluated by relaxing the ions). In the $TbMnO_3$ case, the order of magnitude of the *ab-initio* polarization was found to be in excellent agreement with experiments [87]. Remarkably, at the time of publication, the sign of polarization obtained within DFT was opposite with respect to experiments; indeed, it later turned out [88] that the discrepancy was due to a misunderstanding in the conventions of the experimental settings and an excellent agreement between theory and experiments could be finally obtained.

Within the field of charge-order-induced ferroelectricity, a prototype has emerged: the triangular mixed-valence iron-oxide, $LuFe_2O_4$ [89]. There, the frustrated charge-ordering is such as to lack centrosymmetry: in each FeO bilayer, there is an alternation of iron atoms, with Fe^{2+}:Fe^{3+} ratios of 2:1 and 1:2, therefore giving rise to a polarization within each bilayer. The polarization estimated from first-principles is very large (of the order of 10 $\mu C/cm^2$ in the bilayer). However,

some controversy exists for that material, since it is questioned whether the stacking of the bilayers is such as to produce net ferroelectricity [83] or a global antiferroelectricity with no net polarization [90]. More work (both from theory and from experiments) will be needed in that respect.

Recently, another collinear compound has been studied, Ca_3CoMnO_6 [79,80]. The main *ab-initio* findings were: *i*) a large Co orbital moment, which renders the system similar to an Ising-like chain, with alternating trigonal prismatic Co^{2+} and octahedral Mn^{4+} sites in the spin chain; *ii*) a large calculated polarization (about 1.7 $\mu C/cm^2$), caused by a significant exchange-striction combined with a peculiar $\uparrow\uparrow\downarrow\downarrow$ spin configuration.

Given this general background, in the following sections we will present some examples of *ab-initio* calculations for IMF. In closer detail, we will discuss rare-earth manganites (*cfr.* Sec. 3.1.1) [74, 78] and hole-doped manganites (*cfr.* Sec. 3.1.2) [85] as examples of AFM materials where the spin-arrangements break inversion symmetry, with polarization being due to Heisenberg-like mechanisms. We will conclude the section by discussing some perspectives and open issues in the field.

In what follows, we will mainly show the results of DFT simulations performed using the Vienna Ab-initio Simulation Package (VASP) [91] and the generalized gradient approximation [92] to the exchange-correlation potential. For the construction of the Wannier functions, we used the Full-potential Linearized Augmented Plane-Wave (FLAPW) [93] code in the FLEUR implementation [94]. For a better treatment of correlation effects, the so-called LSDA+U approach [17] (with $U = 4$ eV and $J = 0.9$ eV) was used in the case of hole-doped manganites. For further technical details, as far as computational or structural parameters are concerned, we refer to our original publications [74, 78, 85].

3.1 Highlights on Improper Multiferroics

3.1.1 E-type rare-earth ortho-manganites

Let us start the discussion of ferroelectricity in orthorhombic manganites, $R MnO_3$, by plotting the AFM spin-arrangement characteristic of the E-type $HoMnO_3$. In Fig. 6a we sketch the ions in the MnO_2 plane and highlight the zig-zag spin-chains, typical features of the E-type antiferromagnetism: zig-zag ferromagnetic (FM) spin-up-chains (green atoms in Fig. 6a) are antiferromagnetically coupled to neighboring spin-down-chains (pink atoms in Fig. 6a). The out-of-plane coupling is also AFM. We note that the antiferromagnetically-coupled zig-zag chains lead to a doubling of the conventional $GdFeO_3$-like unit cell (20 atoms, *Pnma* space group) along the *a*-axis. Indeed, the E-type was experimentally observed to be the magnetic ground state in distorted manganites with small ionic radius for the rare-earth ion (*i.e.* $R =$ Ho, ..., Lu) [96,97]. It was shown [12,78] that the stabilization of an $\uparrow\uparrow\downarrow\downarrow$ spin-chain (as the one present in the E-type along the diagonal directions in the *a*-*c* plane, *cfr.* Fig. 6a), is driven by *i*) a relatively small nearest-neighbor exchange coupling constant; *ii*) a large AFM next-nearest-neighbor; *iii*) a quite large magnetic anisotropy so that the spins can be considered as Ising-like.

Why should the E-type magnetic configuration lead to a ferroelectric polarization? This can be rationalized in different (though somewhat inter-connected) ways, depending on the orbitals or

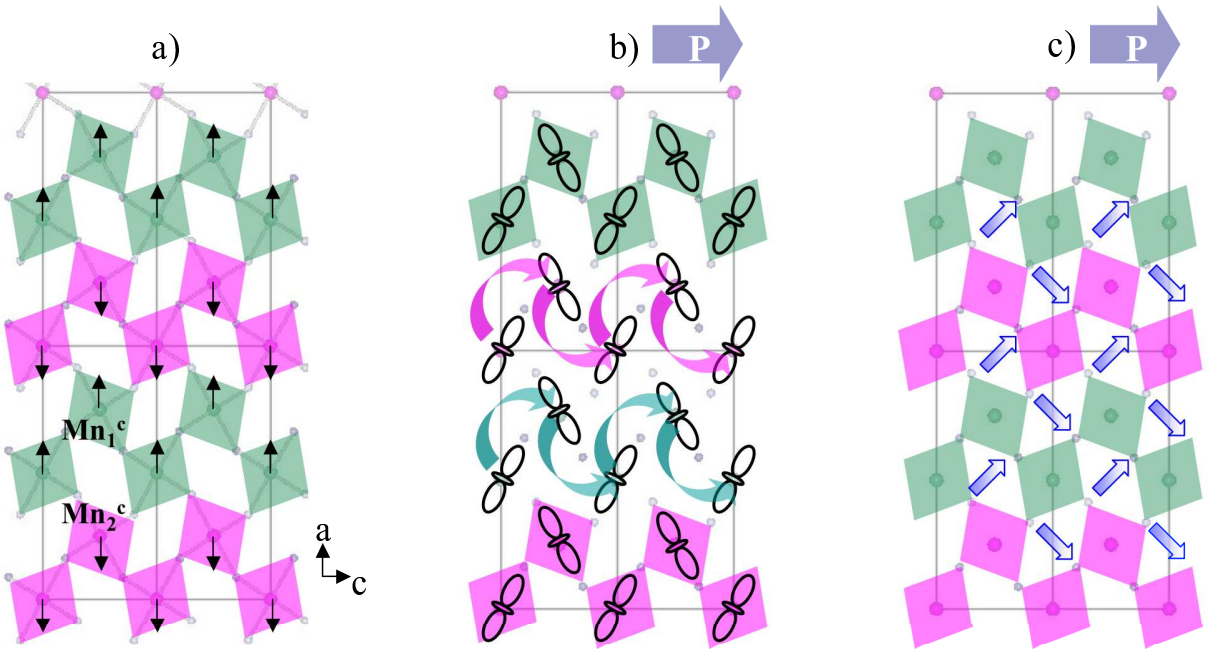

Figure 6: a) Ionic arrangement of AFM-E $HoMnO_3$ in the MnO_2 plane. Green (pink) rhombi denote in-plane projections of MnO_6 octahedra around the up-spin (down-spin) Mn ion. Spin directions indicated by black arrows. b) Schematic orbital-ordering for Mn e_g states. Circular arrows show hopping paths, as induced by the AFM-E spin configuration; green and pink arrows denote asymmetric hoppings for up-spin and down-spin electrons, respectively. c) Schematic local dipoles (denoted by blue arrows) drawn from O^{ap} (bonded to Mn with antiparallel spins) to O^{p} (bonded to Mn with parallel spins). In b) and c), the direction of polarization is also shown.

atoms one focuses on.

Let's start with Mn e_g states. Being Mn in a d^4 electronic configuration, the strong Jahn-Teller effect leads to two large and two small in-plane Mn-O bond lengths, along with a staggered $(3x^2 - r^2)/(3y^2 - r^2)$ orbital-ordering, typical for the class of rare-earth manganites. Within a double-exchange-like picture, this peculiar orbital-ordering (OO) leads to a favored hopping of the electron on the two (out of four nearest neighbors) Mn-sites towards which the orbital is pointing. What is peculiar of the E-type (and different from the conventional A-type in early-rare-earth manganites) is that, out of these two Mn sites, hopping will preferentially occur on the Mn with the spin parallel to the starting site, and not on the other which shows an opposite spin. This "asymmetric" hopping creates a "one-way path" for the electron, schematically shown by the circular arrows in Fig. 6b. At this point, it is clear that the short c axis is a "preferential" direction for the electron, with a well-defined sign for the electron hopping. This mechanism therefore breaks inversion symmetry and opens the way to a ferroelectric polarization P_c.

Another way to explain the direction of polarization is to look at oxygen sites. Again due to the peculiar E-type spin-configuration, there will be two kinds of O sites: those bonded to Mn with parallel spins (labeled as O^p) and those bonded to Mn with antiparallel spins (labeled as O^{ap}). Due to this inequivalency, their electronic structure will be different (even if the ions are frozen into a centrosymmetric "paramagnetic" configuration). This leads to a sort of oxygen "charge-density wave" which can be thought of in terms of a set of ordered dipoles resulting in a net ferroelectric component, again only along the short c-axis (*cfr.* Fig. 6c).

We would now like to make one comment related to ferroelectric switching in IMF. As is well known, in conventional displacive perovskite-like ferroelectrics, the switched state (*i.e.* the one with $-\vec{P}$) is achieved by displacing the ions (with respect to a reference centrosymmetric structure) in the opposite way compared to the $+\vec{P}$ state. However, when asking how to switch $\vec{P}$ in the case of magnetically-driven ferroelectrics, one might guess that some changes in the spin-arrangement (rather than in the ionic arrangement) should be involved. Indeed, from both Fig. 6b and c, it is clear that $\vec{P}$ is switched by changing the direction of half of the spins in the unit cell. For example, if we revert the sign of the two spins in the central part of the unit cell (labelled as Mn_1^c and Mn_2^c in Fig. 6a), then the circular arrows in Fig. 6b will run in the opposite $-c$ direction; similarly, the O-related dipoles of Fig. 6c will also change their sign.

So far, we have taken into account purely "electronic" mechanisms, occurring when considering the ions frozen into their centrosymmetric configuration. However, it is reasonable to expect some ionic relaxations consistent with the imposed E-type spin arrangement. For example, according to a Heisenberg-like magnetostrictive effect, one expects that O^p will try to move so as to gain a "double-exchange"-like energy by maximizing the Mn-O-Mn angle (recall that the energy lowering due to double-exchange is optimal in the ideal 180-degree case), compared to O^{ap} where double-exchange is not relevant. These ionic relaxations break the atomic centrosymmetry and lead to an "ionic" contribution to the total ferroelectric polarization, to be added to the purely electronic one.

On the basis of this introductory background, the interpretation of DFT results for $HoMnO_3$ is quite straightforward. It is however very important to remind that, at variance with model-Hamiltonian studies allowing the qualitative prediction of a selected phenomenon, first-principles

calculations can provide a quantitative estimate as well. Moreover, multiferroics are very complex materials where several competing mechanisms can occur. As such, identifying the strong and prevailing effects can be difficult within a Hamiltonian-modelling approach; on the other hand, all the different mechanisms are taken into account on the same footing within DFT.

We report in Table 1 the relevant properties calculated within DFT, such as: *i*) the Mn-O-Mn angles between parallel (α^p) and antiparallel (α^{ap}) Mn spins, obtained after ionic relaxations in the presence of the E-type spin arrangement; *ii*) the values of the polarization calculated in several different ways: a purely electronic contribution (P_{ele}^{BP}), estimated via the Berry-phase approach, when the ions are clamped in a centrosymmetric *Pnma* configuration; the polarization calculated from the so-called "Point Charge Model" (P_{ion}^{PCM}), with the ions relaxed in the ferroelectric configuration, using "nominal" ionic values for the charges (*i.e.* 3+ on Mn and Ho and 2− on the O); the total (ionic + electronic) polarization in the relaxed ionic arrangement, calculated according to the Berry-phase approach (P_{tot}^{BP}); *iii*) the Born effective charges, *i.e.* the (3,3) components of the Z^* tensor for some relevant atoms: Z^*(Mn), $Z^*(O^p)$ and $Z^*(O^{ap})$. We recall that the $Z^*_{3,3}$ elements are estimated by displacing the selected ion along the c direction by a small amount (typically about 0.01 Å or less) and evaluating the change in the Berry-phase polarization along the same c axis.

When focusing on the Mn-O-Mn angles, we indeed note that the angle between Mn with parallel spins is much larger than that where spins are antiparallel, reflecting the efficiency of relaxations driven by double-exchange mechanisms. As for polarization, several remarks are in order: *i*) one might naively expect a magnetically-induced mechanism to be "weak". However, this is contradicted by the purely electronic polarization, which is noticeably large. Moreover, this is one order of magnitude bigger than what was estimated in the case of spin-spirals ($\leq\sim 0.1$ μC/cm^2): this reflects the efficiency of the Heisenberg vs. DM term in breaking inversion symmetry. *ii*) A similar consideration holds for the total polarization. Exchange-strictive effects due to the symmetric Heisenberg term result in ionic displacements which cooperate with the purely electronic polarization, summing up to the appreciable value of 6 μC/cm^2.

So far, we have discussed the prototypical case of $HoMnO_3$; however, as previously mentioned, the E-type is the magnetic ground state for many distorted manganites [97] and it is therefore interesting to investigate how the relevant properties (with a focus on polarization) change as

Mn-O-Mn (°)		P (μC/cm^2)			$Z^*_{3,3}$ (e^-)		
α^p	α^{ap}	P_{ele}^{BP}	P_{ion}^{PCM}	P_{tot}^{BP}	Z^*(Mn)	$Z^*(O^p)$	$Z^*(O^{ap})$
145.3	141.9	2.1	3.5	6.1	3.8	-2.6	-3.5

Table 1: Relevant calculated properties in $HoMnO_3$. First two columns: Mn-O-Mn angles, broken down into values for the case of parallel (α^p) and antiparallel (α^{ap}) spin. Third to fifth columns: polarization values calculated when considering only the electronic polarization in the original centrosymmetric structure (P_{ele}^{BP}), or only the PCM value upon structural relaxation (P_{ion}^{PCM}) and the total Berry-phase polarization for the relaxed ionic coordinates (P_{tot}^{BP}). Sixth to eighth columns: (3,3) components of the Born effective charge tensors, for Mn ions (Z^*(Mn)) and the two inequivalent in-plane oxygens ($Z^*(O^p)$ and $Z^*(O^{ap})$).

a function of the rare-earth [78]. Recall that the rare-earth cation has primarily the effect of increasing the octahedral $GdFeO_3$-like tilting as a result of reducing the ionic size when moving, say, from La to Lu; on the other hand, the Jahn-Teller-like distortions are weakly affected by the rare-earth atom [78, 97]. The structural modifications (relative to the Mn-O-Mn angles) have in turn important consequences on the magnetic and dipolar order. As for the former, we have shown [78] that the first-nearest-neighbor ferromagnetic exchange-coupling constant progressively weakens upon decreasing the ionic radius, whereas the strong second-nearest-neighbor AFM exchange constant is more or less constant along the series. This implies the progressive change of the magnetic ground-state from A-type (in early rare-earth manganites) to E-type (in late rare-earth manganites), going through the intermediate region (R = Tb, Dy) where the spin-spiral occurs as ground state. What happens to polarization? To perform a complete investigation of the ferroelectric properties as a function of the octahedral tilting, we have imposed the E-type magnetic state on all the rare-earth manganites, irrespective of the actual magnetic ground-state. This is a typical example of a "computer-experiment": within DFT, at variance with real experimental samples, one can impose several different structural, electronic or magnetic configurations (not necessarily the ground states) to have clear insights on specific phenomena or to separate several competing effects.

What we focus on here is the construction of Wannier functions (WF) [22, 95] for the Mn e_g, Mn t_{2g} and O p band manifolds and on the position of the WF center with respect to the relative ionic site. The difference between the polarization calculated according to the point-charge-model and via the Berry-phase approach is commonly referred to as the "anomalous" contribution to polarization. As such, it reflects somewhat the deviation from a purely ionic state or, equivalently, highlights the covalent character of the atomic bonds and, in turn, of the electronic structure. Moreover, we also recall that the polarization via the Berry-phase approach is equivalent to the sum of the displacement of the center of each WF from the position of the corresponding ion plus PCM contribution. The latter was shown [78] to be rather unaffected by the R-ion, with a value $P_{ion}^{PCM} \sim 2\ \mu C/cm^2$.

In Fig. 7 we report the different contributions to the total polarization in the spin-up channel coming from the displacements of the WF centers for the Mn e_g, Mn t_{2g} and O p, along with their sum (leading to the spin-up "anomalous contribution"). We note that Mn t_{2g} states contribute in an opposite way with respect to Mn e_g and O p states, the total P having the same sign as the two latter contributions. Moreover, it is quite clear that, whereas the O p and Mn t_{2g} depend relatively little on the rare-earth ions, the e_g contribution is very sensitive to structural distortions. Indeed, for a hypothetical $LaMnO_3$ in the E-type spin configuration, there would be a total polarization (coming from twice the spin-up contribution shown in Fig. 7 plus the PCM term), summing up to a value greater than 10 $\mu C/cm^2$! This confirms the strong sensitivity of the e_g states to the Mn-O-Mn angle: as reported in Ref. [78], the hopping integral strongly decreases when moving from La to Lu, consistent with a progressively reduced band width. Whereas promising ways to increase P would appear in the early rare-earth manganites (but where unfortunately the magnetic ground state is the (paraelectric) A-type AFM), the total polarization seems pretty much "saturated" to a value of the order of 6 $\mu C/cm^2$ in going from Ho to Lu.

We would like to comment now on the comparison with experiments. First of all, we remark

that several problems exist with the experimental synthesis of the late R manganites: indeed, the stable structure is hexagonal, not orthorhombic [97, 98]. Modern growth techniques, such as high-pressure high-temperature synthesis, can do the job and synthesize ortho-manganites for late rare-earths, leading however not to single-crystals but rather to polycrystalline samples. This poses problems for the exact evaluation of ferroelectric polarization, due to possible different orientations of the polarization vector in the polycrystalline grains. To our knowledge, there exists several values in the literature. Lorenz *et al.* [99] reported $P \sim 0.001$ μC/cm^2 for $HoMnO_3$, *i.e.* a value smaller by two or three orders of magnitudes than our *ab-initio* estimates. On the other hand, a much larger value was recently reported in AFM-E $TmMnO_3$ [100]: a lower bound of (unsaturated) polarization of about 0.15 μC/cm^2 was measured, in much better agreement with our theoretical values. This is especially so, since Pomjakushin *et al.* [100] suggested that the threshold of 1 μC/cm^2 could be easily achieved in the case of single crystals. In this respect, we would also like to remark that the values discussed so far are calculated within a bare DFT approach. It is however well known that DFT fails in accurately modelling strong correlation effects, which might occur in manganites. However, the inclusion of an Hubbard-like correction according to the so-called LSDA+U approach for Mn d states in $HoMnO_3$, lead to values of the polarization all larger than 1–2μC/cm^2 for $U \leq 8$ eV. Recently, in Ref. [101], the authors reported a theoretical model in the context of electromagnon excitations in $RMnO_3$. One of the outcome was the estimate of the polarization in E-type manganites based on optical absorption data measured for $TbMnO_3$ in the spiral-phase: P was found to be of the order of 1 μC/cm^2, therefore large and compatible with our theory estimates. Though some controversy is still present, there are more and more confirmations that the polarization in E-type is much higher than in the spiral phases studied so far, consistently with the generally accepted argument that magnetostrictive effects in the symmetric Heisenberg-like exchange should be stronger than in the antisymmetric DM part.

3.1.2 Half-doped manganites: $La_{0.5}Ca_{0.5}MnO_3$

Hole-doped manganites (*i.e.* $A_{1-x}B_xMnO_3$ where A = La, Pr, ... and B = Ca, Sr, ...) show a rich physics, with exciting phenomena ranging from charge-ordering to half-metallicity, from colossal magnetoresistance to exotic phase diagrams, from orbital-ordering to metal-insulator transitions. We will here discuss the possibility that hole-doped manganites, with a hole-concentration $x \sim 0.5$, might also become ferroelectric and, therefore, multiferroic.

$La_{0.5}Ca_{0.5}MnO_3$ (denoted in the following as LCMO) is a very complex system from many points of view (electronic, structural, magnetic, etc.) and, despite the many decades of work since the first seminal paper [102], its properties have not been clearly elucidated. In particular, even the exact ionic coordinates and related symmetries are still debated. Two main models have been proposed so far: *a*) the first one, proposed by Radaelli *et al.* [103], is based on a site-centered charge-ordered (SC-CO) Mn^{3+}/Mn^{4+} checkerboard arrangement in the MnO_2 plane (see Fig. 8c), in which the octahedron around Mn^{3+} is Jahn-Teller-like distorted, whereas the octahedron around Mn^{4+} is rather regular; *b*) the second one, proposed by Rodriguez *et al.* [104] and referred to as a bond-centered charge-ordered (BC-CO), is based on a structural dimerization of Mn ions (all in a d^4 configuration). This leads to a peculiar OO: at variance

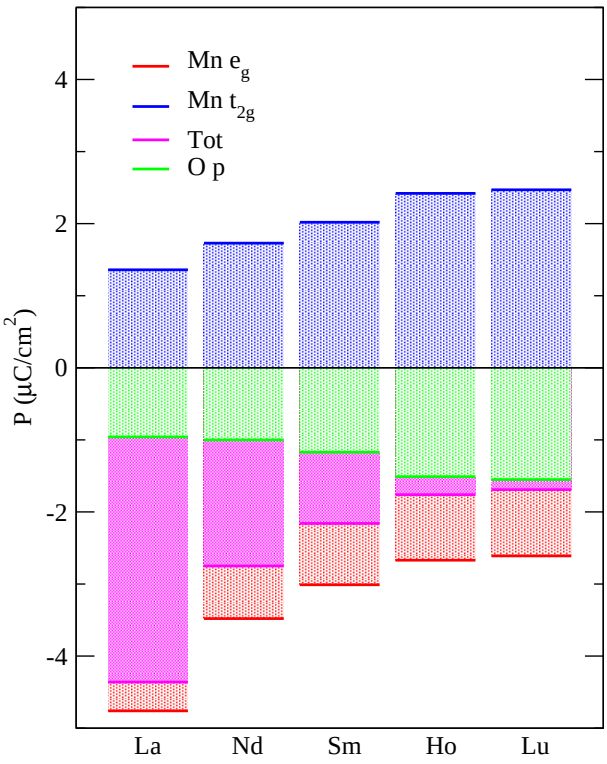

Figure 7: Different up-spin contributions to the "anomalous" term in the polarization (in μC/cm^2) as derived from WF centers: Mn e_g (red), Mn t_{2g} (blue), O p (green) and total (magenta) as a function of the rare-earth ion (R = La, Nd, Sm, Ho, Lu).

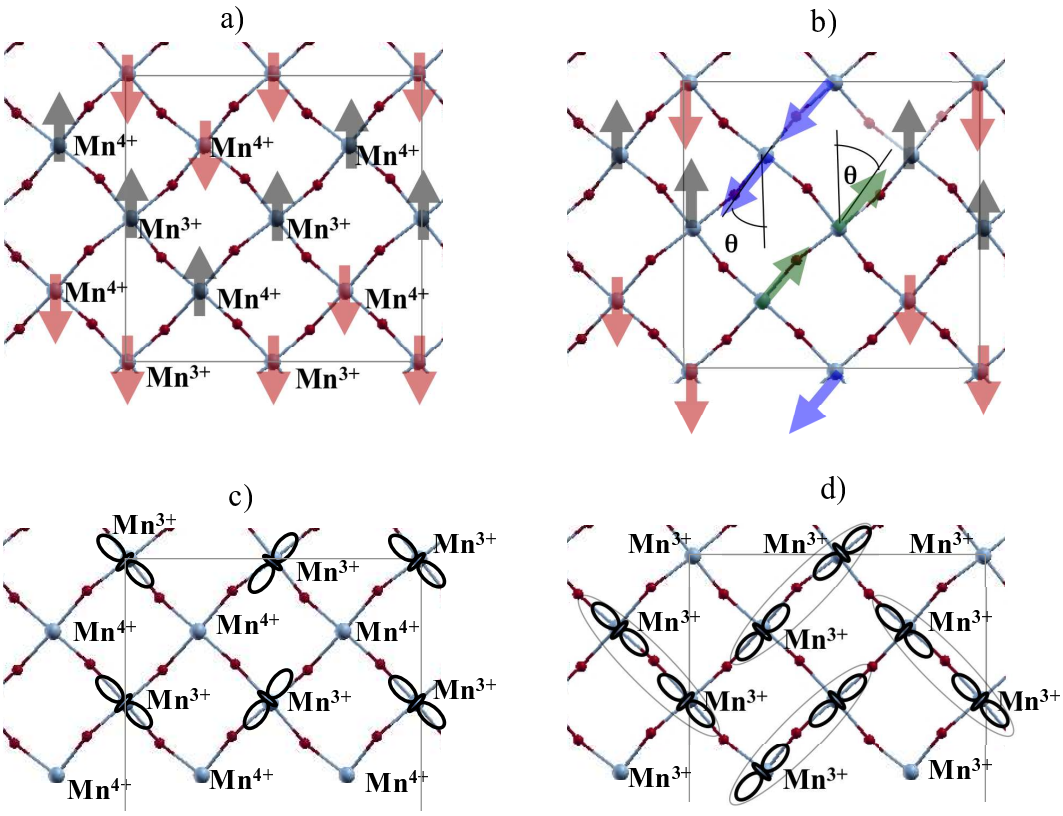

Figure 8: a) Checker-board arrangement of Mn^{3+} and Mn^{4+} in the MnO_2 plane in the SC-CO structure. The AFM-CE magnetic configuration is shown by double zigzag up (black arrows) and down (red arrows) spin chains. b) Sketch of the θ rotation: the spins on two neighboring Mn atoms in the up-spin chain are rotated clockwise by θ (green arrows), along with two corresponding spins on neighboring Mn in the down-spin chain rotated clockwise by θ (blue arrows). c) The schematic orbital-ordering in the SC-CO structure: ideally, there should be an elongated Jahn-Teller-like e_g orbital centered on the Mn^{3+} site and no-e_g-like charge on the Mn^{4+} site. d) The schematic OO in the BC-CO structure: the two Mn ions in the dimer show their e_g orbitals oriented one towards each-other. ZP units (*i.e.* two Mn and the O in-between) are highlighted by ellipses.

with the staggered OO previously mentioned for $LaMnO_3$, here the filled Mn e_g orbitals in the dimer point one towards each other. With respect to the mother compound, $LaMnO_3$, there is one extra-hole every two Mn: the (spin-polarized) hole is believed to be located on the central O in between the two Mn. This peculiar unit (formed by two Mn and the O in between) is often referred to as "Zener-polaron" (ZP) [105,106], after the Zener double exchange mechanism which should be enhanced here (see Fig. 8d).

As far as the magnetic spin-configuration is concerned, the so-called CE-type AFM (*i.e.* double zig-zag spin chains in the MnO_2 plane, *cfr.* Fig. 8a) has been proposed as ground-state.

We will here focus on two different mechanisms which might lead to improper ferroelectricity in LCMO:

- The first one is based on breaking inversion symmetry in the spin-chains through a rotation

(by an angle θ) of the spins on two nearest-neighbor Mn in the up zigzag chain, along with a corresponding rotation of two spins in the down spin-chain (*cfr.* Fig. 8b), so as to keep a global AFM character. This follows the theoretical proposal put forward by Efremov *et al.* [107], who first suggested the possibility of multiferroicity in manganites. According to Ref. [107], such rotation should progressively lead from a fully SC-CO (in the ideal CE-type, $\theta = 0°$) to a fully BC-CO for $\theta = 90°$ (where the dimerization process driven by spin ordering is maximized). Efremov *et al.* predicted that, in both the extreme cases, $\theta = 0°$ and $\theta = 90°$, the polarization should vanish: for $\theta = 0°$, the checkerboard arrangement should be fully centrosymmetric (both structurally and electronically), whereas for $\theta = 90°$ the Mn should not show any charge-disproportionation. However, for in-between values of θ, the intermediate SC-CO/BC-CO should lead to a small charge-disproportionation and, therefore, to inequivalent Mn (at variance with the ZP state and reminiscent of the site-centered CE-type). In this case, inversion symmetry would be broken by spin-dimerization, therefore paving the way to ferroelectricity;

- The second mechanism occurs in the structure experimentally proposed by Rodriguez *et al.* [104]. The related unit cell shows a "*structural*" Mn-Mn dimerization and implies a realization of a BC-CO, not invoking (non-collinear) magnetic mechanisms as in the previous case, but rather thanks to electronic rearrangement — such as OO — following the structural distortions. Still, in this case, our mechanism for multiferroicity is once more a (collinear) magnetically induced mechanism based on the inequivalency of some specific oxygen atoms, as will be detailed below.

Due to the large unit-cell (80 atoms, needed to simulate the CE-type AFM ordering, along with a checkerboard arrangement of La and Ca cations) and the need of non-collinear spin magnetism (needed to simulate finite values of θ), the computational cost of these simulations is very high. For this reason, the ionic positions were not optimized within DFT, but were rather kept frozen in the structure proposed either by Radaelli [103] or by Rodriguez [104], labelled in what follows as LT-M or by LT-O, respectively. Unfortunately, the lack of ionic minimization forbids any DFT prediction of the actual structural and magnetic ground-state from total-energy arguments; this calls for future studies. From our calculated values for unrelaxed structures, it seems that the CE with SC-CO is the phase showing lowest total energy; however, for example, the SC-CO state with a rotation $\theta = 45°$, is higher in energy by only ~ 4 meV/Mn. One can therefore conjecture that, in real samples, there might be a coexistence of nanoscale regions with different magnetic structures (*i.e.* with zero and finite θ values).

Before discussing the relevant ferroelectric properties, let us mention some general features in the electronic structures of the LT-M and LT-O systems, both in the CE-type AFM spin configuration (*i.e.* $\theta = 0$). In Fig. 9 we show the isolines of the electronic charge plotted in the energy region where the Mn e_g states are located. It is clear that in the LT-M (Fig. 9a) the shape of the e_g electronic cloud, centered on the "nominal" Mn^{3+}, is markedly elongated towards the neighboring Mn^{4+} with parallel spins. On the other hand, the Mn^{4+} show a very isotropic distribution of the charge. The situation is different in the LT-O structure (Fig. 9b), where the OO clearly shows the e_g orbitals forming "dimers" with their charge distribution pointing one towards the other, as driven by the underlying ionic configuration. Let us mention a note on the

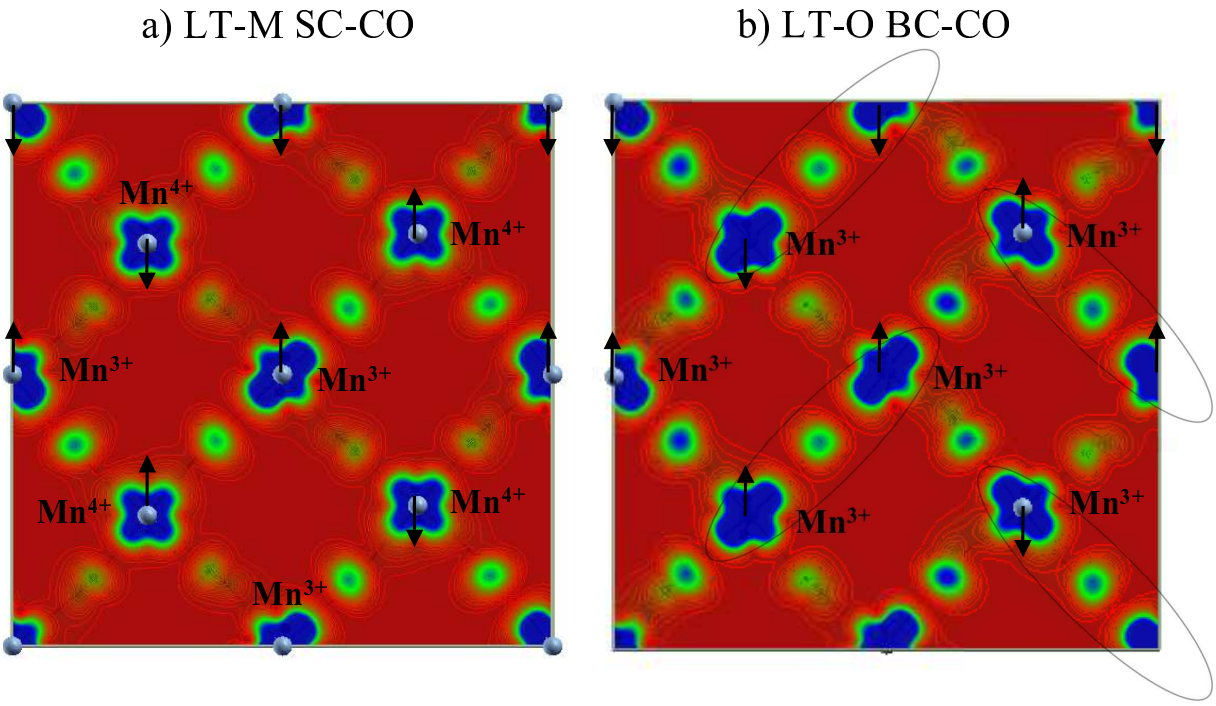

Figure 9: Isolines of the e_g charge in a) the LT-M SC-CO and b) the LT-O BC-CO structures. Red (blue) lines marks the minimum (maximum) charge, through the intermediate green lines. In a), black arrows mark the Mn spin directions. In b), ZP are highlighted.

CO: consistently with previous reports, the actual charge-disproportionation in LCMO within DFT is of the order of only 0.1–0.2 electrons in the LT-M SC-CO, at variance with the ideal situation of "full" charge disproportionation, where the e_g electron cloud should be completely distributed around the Mn^{3+}, with no-charge on the Mn^{4+}. In this sense, the calculated OO in the LT-M (*cfr.* Fig. 9a) is different from the nominal situation (*cfr.* Fig. 8c) with clear signatures of e_g charge also around the Mn^{4+}. We remark, however, that the small charge-disproportionation detected in the LT-M structure becomes really negligible (<0.02 electrons) in the LT-O BC-CO; this suggests that it is still meaningful to consider the LT-M → LT-O transition as a corresponding SC-CO → BC-CO transition.

Let's now consider what happens in the LT-M structure upon increasing θ from the initial zero-value: our calculated electronic structures (not shown, see Ref. [85]) indicate a decreasing e_g band-width and a related increasing band-gap. This can be rationalized by comparing the spin-arrangement with finite θ with the original CE-type. Upon spin rotation, the e_g electron — which could hop equivalently on the two nearest-neighbor Mn^{4+} on both sides along the spin-chain in the CE-AFM phase — will now preferentially hop on the Mn^{4+} which shows a parallel spin, since hopping in the other direction is prevented by the spin misalignment. This effect would rather lead to a decreased hopping and to a reduced e_g band-width, at variance with our findings. However, one needs to consider that, for $\theta \neq 0$, there will be an increasing probability to hop on the neighboring spin-chain (prevented by opposite spin configuration in the CE-AFM phase). Overall, there will be therefore an increased hopping integral, consistently with our findings and with Hamiltonian-modelling studies, as well [85].

For our purposes, the most important finding is that a finite θ in the LT-M induces a rather large polarization, as shown in Table 2 (first line), with an increasing parabolic trend of P vs. θ. We note that this is a purely electronic polarization, since the ions are fixed in their centrosymmetric arrangement [103]. The Heisenberg-like symmetry breaking — as driven by spin-rotation — is therefore confirmed as an efficient tool to induce large ferroelectricity (recall that spin-orbit coupling and the related DM interaction is neglected in the present context).

We will now focus on the calculated values of P in the LT-O structure (see Table 2) and start the discussion for the $\theta = 0$ case. Without any magnetic ordering imposed and as determined experimentally, the LT-O structure shows a $P2_1nm$ space group: this implies that some in-plane oxygens are structurally equivalent (shown in the same color in Fig. 10), due to the 2_1 screw symmetry. However, when imposing the AFM-CE spin-configuration, the Oxygen equivalency is lifted: there is an alternation of O^p bonded to two parallel spins and of O^{ap} bonded to two antiparallel spins. This is sufficient to give rise to ferroelectricity in the direction shown in Fig. 10. Remarkably, the induced polarization reaches the surprisingly large value of several $\mu C/cm^2$. To further verify that a magnetically-induced mechanism is the source of the ferroelectricity, we have also performed a θ-like rotation of the spin dimers, similar to the previous case of the LT-M (*cfr.* Fig. 8 b)). In this case, upon spin-rotation, the inequivalency of the Oxygens crossing the 2_1 axis is reduced. In the extreme situation, $\theta = 90°$, all the O atoms are now bonded to two Mn with perpendicular spins: in this configuration, they all look equivalent and the source of polarization vanishes. Indeed, DFT calculations confirm that this is the case (*cfr.* Table 2). In summary, our DFT results (both from $HoMnO_3$ and LCMO) offer a confirmation that the O inequivalency is an efficient handle to achieve and/or tune a large ferroelectric response.

3.2 Problems and perspectives in Improper multiferroics

As indicated by the huge interest in the last few years, magnetically-driven ferroelectrics, with ortho-$TbMnO_3$ taken as prototype, are with no doubt an exciting class of materials. However, there are a few bottlenecks which prevent their use in large-scale applications: *i*) their polarization is generally very small (≤ 0.1 μC/cm^2); *ii*) their ordering temperature is very low (of the order of few tens of K); *iii*) being globally antiferromagnets, their net magnetization is always zero (a ferromagnetic spin ordering alone cannot break inversion symmetry!). In this respect, we will certainly see some activity in future years to get rid of these problems.

As shown in this review, at least point *i*) can be beautifully overcome when considering Heisenberg-like exchange-striction, as shown in E-type manganites. The ordering temperature of the latter is, however, extremely low ($T_N(HoMnO_3) \sim 26$ K). One possibility to increase the ordering

	0°	22.5°	45°	67.5°	90°
LT-M	0.0	0.19	0.66	1.56	2.70
LT-O	7.18	6.62	5.13	2.84	0.0

Table 2: Berry-phase polarization (in μC/cm^2) calculated in the LT-M and LT-O structure as a function of spin-rotation angles θ (first line).

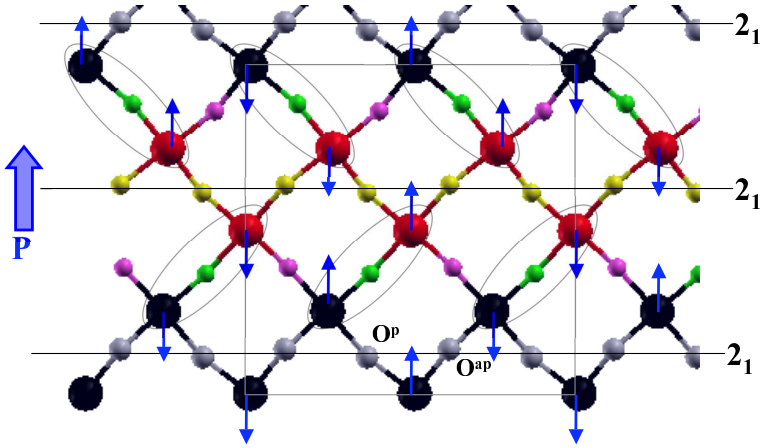

Figure 10: Atomic configuration in the MnO_2 plane of the LT-O structure: symmetry-equivalent atoms are marked in the same color. Note that red and black spheres mark Mn atoms: despite being symmetry-inequivalent, the two kinds of Mn are only marginally different from the electronic point of view, with small differences in the Mn-O bond-lengths (see Ref. [104].). Horizontal lines mark the two 2_1 screw axes in the unit cell, crossing the O atoms (marked as grey and yellow). The blue arrows on the Mn ions denote the spin directions in the AFM-CE spin configuration: when considering the spin-directions, the grey atoms (structurally equivalent by symmetry) become electronically different: they are alternatively bonded to two parallel Mn spins and to two anti-parallel spins (see labels on two selected oxygens).

temperature without losing the non-centrosymmetric Heisenberg-like exchange-striction is to consider rare-earth nickelates [86] (for example, $T_N(HoNiO_3) = 145$ K, $T_N(LuNiO_3) = 130$ K, etc.). Nickelates are rather complex materials, with several important issues still under debate, including the origin of their metal-insulator transition as well as their spin configuration. As for the latter, both non-collinear and collinear spin-arrangements have been put forward from neutron diffraction studies [108, 109]. In addition, nickelates show a charge-disproportionation: Ni ions, in the nominal 3+ valence-state, split into two groups of Ni^{2+} and Ni^{4+} [110]. This adds one degree of freedom to achieve ferroelectricity. For example, as suggested in Ref. [111], one of the proposed magnetic configurations shows, along the [111] direction, a sequence of Ni^{2+}-Ni^{4+}-Ni^{2+}-Ni^{4+} as for charge-ordering and a sequence of $\uparrow\uparrow\downarrow\downarrow$ planes as for spin-ordering. The combination of spin and charge-ordering would break centrosymmetry, leading to a polarization along the [111] direction. Another spin-configuration, proposed by experiments, seems to be very similar to the E-type in $HoMnO_3$, the only difference being the stacking of TMO_2 (TM = Mn, Ni) planes: whereas the out-of-plane coupling is always AFM in $HoMnO_3$, in nickelates there are NiO_2 alternatively coupled ferromagnetically and antiferromagnetically. However, the different out-of-plane stacking does not destroy the mechanism for polarization, induced in a way very similar to $HoMnO_3$. Our preliminary calculations [86] show that the two mentioned collinear magnetic ground-states in monoclinic $RNiO_3$ (R = Ho, Lu) are basically degenerate (*i.e.* the differences in total energies are below our numerical uncertainty). Consistently with a Heisenberg-driven mechanism, both spin-configurations give rise to a large polarization (of the order of few $\mu C/cm^2$) along different directions, suggesting nickelates as a new and interesting class of magnetically-driven multiferroics.

Going back to the bottlenecks mentioned above, point *iii*) might be overcome by considering magnetite. In this review, we have discussed so far a few examples where spin-ordering is a necessary ingredient to break inversion symmetry. However, there are materials in which the polarization is induced purely by charge-ordering, such as $LuFe_2O_4$ and Fe_3O_4 below the Verwey transition temperature (*i.e.* corresponding to the metal-insulator transition, $T_V \sim 120$ K). In magnetite, the spin-arrangement is ferrimagnetic (*i.e.* tetrahedral and octahedral Fe sites show up and down spin, respectively). The role of magnetism, however, does not seem to be relevant for polarization. Magnetite is a complex and controversial system: the Fe^{2+}/Fe^{3+} charge ordering pattern on octahedral iron sites is still under debate [112, 113]. However, the Cc symmetry has been proposed by diffraction studies and confirmed from first-principles to be the ground state [114]. In the Cc case, octahedral Fe sites, form a corner-sharing tetrahedron network: 75% of the tetrahedra show the so-called "3:1" pattern (meaning that, in each tetrahedron, 3 sites are Fe^{2+} and one is Fe^{3+} or vice versa), whereas 25% show a 2:2 pattern (meaning that 2 sites are Fe^{2+} and two are Fe^{3+} in the tetrahedron). It happens that the Cc is non-centrosymmetric; indeed, our DFT calculations [84] show the polarization induced by charge-ordering to be of the order of few $\mu C/cm^2$, suggesting magnetite to be the first improper multiferroic known to mankind.

4 Summary and Conclusions

In summary, we have presented some examples which show the power of DFT-based methods in the field of multiferroic materials. This includes: *i*) rationalizing experimental observations in known multiferroics, *ii*) designing new (artificial) multiferroics with optimized properties (larger ferroelectric polarization, strong ferromagnetism, higher ordering temperatures, etc.), and *iii*) proposing and quantifying novel microscopic mechanisms, based on electronic degrees of freedom, which potentially lead to ferroelectricity in magnetic transition metal oxides.

It is apparent that the field of proper magnetic ferroelectrics has a relatively long history: many of these materials have already been studied in the 1960s or later, but have only recently been rediscovered. Due to substantial advancements in experimental synthesis and characterization techniques on one side, and the availability of powerful computational methods together with new theoretical approaches on the other side, substantial progress in understanding these materials has been achieved during recent years. Similar to the the case of non-magnetic ferroelectrics, first-principles calculations have shown a remarkably high degree of accuracy, reliability, and predictive capability for the class of proper multiferroics. Nevertheless, many open questions still remain, in particular how to achieve large polarization, large magnetization, and strong magneto-electric coupling above room temperature, or what mechanisms for coupling between magnetic and ferroelectric properties do exist in these materials.

On the other hand, the field of DFT calculations for improper multiferroics is only a couple of years old. As such, it is not clear at the moment how accurate the predictive capabilities of current DFT approaches are for relevant quantities such as structural or electronic properties and, most importantly, polarization. On the experimental side, the synthesis of some compounds (*i.e.* as shown for ortho-manganites with late rare-earth ions) is not under full control, making the

theory-experiment comparison rather complicated. On the modelling side, the role of electronic correlations (where DFT often shows its limits) is certainly more relevant in improper than in proper magnetic ferroelectrics. In this respect, future developments on the theory side (*i.e.* invoking novel exchange-correlation functionals to better describe many-body effects) are desirable. As such, a strong interaction with the experimental and model-Hamiltonian communities active in the field, as well as the extension of DFT studies to a much larger set of materials (showing different microscopic mechanisms or simply different chemical, structural, or electronic properties), will be necessary to achieve a satisfactory qualitative and quantitative description of the complex physics at play in improper multiferroics.

Acknowledgements

Part of the research leading to the presented results has received funding from the European Research Council under the EU Seventh Framework Programme (FP7/2007-2013)/ERC grant agreement n. 203523. C.E. acknowledges support by Science Foundation Ireland under Ref. SFI-07/YI2/I1050.

References

[1] P. Hohenberg and W. Kohn, *Inhomogeneous electron gas*, Phys. Rev. **136**, B864 (1964).

[2] W. Kohn and L. J. Sham, *Self-consistent equations including exchange and correlation effects*, Phys. Rev. **140**, A1133 (1965).

[3] Richard M. Martin, *Electronic structure*, Cambridge University Press, 2004.

[4] Nicola A. Spaldin and Manfred Fiebig, *The renaissance of magnetoelectric multiferroics*, Science **309**, 391 (2005).

[5] H. Schmid, *Multi-ferroic magnetoelectrics*, Ferroelectrics **162**, 317 (1994).

[6] Hans Schmid, *On a magnetoelectric classification of materials*, Int. J. Magnetism **4**, 337 (1973).

[7] Craig J. Fennie and Karin M. Rabe, *Ferroelectric transition in $YMnO_3$ from first principles*, Phys. Rev. B **72**, 100103(R) (2005).

[8] G. A. Smolenskii and I. E. Chupis, *Ferroelectromagnets*, Sov. Phys. Usp. **25**, 475 (1982).

[9] Manfred Fiebig, *Revival of the magnetoelectric effect*, J. Phys. D: Appl. Phys. **38**, R123 (2005).

[10] W. Eerenstein, N. D. Mathur, and J. F. Scott, *Multiferroic and magnetoelectric materials*, Nature **442**, 759 (2006).

[11] D. I. Khomskii, *Multiferroics: Different ways to combine magnetism and ferroelectricity*, J. Magn. Magn. Mater. **306**, 1 (2006).

[12] Sang-Wook Cheong and Maxim Mostovoy, *Multiferroics: a magnetic twist for ferroelectricity*, Nature Materials **6**, 13 (2007).

[13] R. Ramesh and N. A. Spaldin, *Multiferroics: progress and prospects in thin films*, Nature Materials **6**, 21 (2007).

[14] Nicola A. Hill, *Density functional studies of multiferroic magnetoelectrics*, Annu. Rev. Mater. Res. **32**, 1 (2002).

[15] Claude Ederer and Nicola A. Spaldin, *Recent progress in first-principles studies of magnetoelectric multiferroics*, Current Opinion in Solid State and Materials Science **9**, 128 (2005).

[16] Vladimir I. Anisimov, Jan Zaanen, and Ole K. Andersen, *Band theory and Mott insulators: Hubbard U instead of Stoner I*, Phys. Rev. B **44**, 943 (1991).

[17] Vladimir I. Anisimov, F. Aryasetiawan, and A. I. Liechtenstein, *First-principles calculations of the electronic structure and spectra of strongly correlated systems: the LDA+U method*, J. Phys.: Condens. Matter **9**, 767 (1997).

[18] D. Hobbs, G. Kresse, and J. Hafner, *Fully unconstrained noncollinear magnetism within the projector augmented-wave method*, Phys. Rev. B **62**, 11556 (2000).

[19] A. H. Mac Donald, W. E. Pickett, and D. D. Koelling, *A linearised relativistic augmented-plane-wave method utilising approximate pure spin basis functions*, J. Phys. C **13**, 2675 (1980).

[20] R. D. King-Smith and David Vanderbilt, *Theory of polarization of crystalline solids*, Phys. Rev. B **47**, R1651 (1993).

[21] Raffaele Resta, *Macroscopic polarization in crystalline dielectrics: the geometric phase approach*, Rev. Mod. Phys. **66**, 899 (1994).

[22] Nicola Marzari and David Vanderbilt, *Maximally localized generalized Wannier functions for composite energy bands*, Phys. Rev. B **56**, 12847 (1997).

[23] Ronald E. Cohen, *Origin of ferroelectricity in perovskite oxides*, Nature **358**, 136 (1992).

[24] N. A. Hill, *Why are there so few magnetic ferroelectrics?*, J. Phys. Chem. B **104**, 6694 (2000).

[25] Alessio Filippetti and Nicola A. Hill, *Coexistence of magnetism and ferroelectricity in perovskites*, Phys. Rev. B **65**, 195120 (2002).

[26] M. Ghita, M. Fornari, D. J. Singh, and S. V. Halilov, *Interplay between A-site and B-site driven instabilities in perovskites*, Phys. Rev. B **72**, 054114 (2005).

[27] Nicola A. Hill and Karin M. Rabe, *First-principles investigation of ferromagnetism and ferroelectricity in bismuth manganite*, Phys. Rev. B **59**, 8759 (1999).

[28] Ram Seshadri and Nicola A. Hill, *Visualizing the role of Bi 6s "lone pairs" in the off-center distortion in ferromagnetic $BiMnO_3$*, Chem. Mater. **13**, 2892 (2001).

[29] J. B. Neaton, C. Ederer, U. V. Waghmare, N. A. Spaldin, and K. M. Rabe, *First-principles study of spontaneous polarization in multiferroic $BiFeO_3$*, Phys. Rev. B **71**, 014113 (2005).

[30] P. Ravindran, R. Vidya, A. Kjekshus, H. Fjellvag, and O. Eriksson, *Theoretical investigation of magnetoelectric behavior in $BiFeO_3$*, Phys. Rev. B **74**, 224412 (2006).

[31] B. B. van Aken, T. T. M. Palstra, A. Filippetti, and N. A. Spaldin, *The origin of ferroelectricity in magnetoelectric $YMnO_3$*, Nature Materials **3**, 164 (2004).

[32] Claude Ederer and Nicola A. Spaldin, *Origin of ferroelectricity in the multiferroic barium fluorides $BaMF_4$: A first principles study*, Phys. Rev. B **74**, 024102 (2006).

[33] Satadeep Bhattacharjee, Eric Bousquet, and Philippe Ghosez, *Engineering multiferroism in $CaMnO_3$*, Phys. Rev. Lett. **102**, 117602 (2009).

[34] James Rondinelli, Aaron S. Eidelson, and Nicola A. Spaldin, *Non-d^0 Mn-driven ferroelectricity in antiferromagnetic $BaMnO_3$*, arXiv:0901.3333 (2009).

[35] S. V. Kiselev, R. P. Ozerov, and G. S. Zhdanov, *Detection of magnetic order in ferroelectric $BiFeO_3$ by neutron diffraction*, Sov. Phys. Dokl. **7**, 742 (1963).

[36] James R. Teague, Robert Gerson, and W. J. James, *Dielectric hysteresis in single crystal $BiFeO_3$*, Solid State Commun. **8**, 1073 (1970).

[37] P. Fischer, M. Polemska, I. Sosnowska, and M. Szymański, *Temperature dependence of the crystal and magnetic structure of $BiFeO_3$*, J. Phys. C **13**, 1931 (1980).

[38] I. Sosnowska, T. Peterlin-Neumaier, and E. Streichele, *Spiral magnetic ordering in bismuth ferrite*, J. Phys. C **15**, 4835 (1982).

[39] J. Wang, J. B. Neaton, H. Zheng, V. Nagarajan, S. B. Ogale, B. Liu, D. Viehland, V. Vaithyanathan, D. G. Schlom, U. V. Waghmare, N. A. Spaldin, K. M. Rabe, M. Wuttig, and R. Ramesh, *Epitaxial $BiFeO_3$ multiferroic thin film heterostructures*, Science **299**, 1719 (2003).

[40] K. J. Choi, M. Biegalski, Y. L. Li, A. Sharan, J. Schubert, R. Uecker, P. Reiche, Y. B. Chen, X. Q. Pan, V. Gopalan, L.-Q. Chen, D. G. Schlom, and C. B. Eom, *Enhancement of ferroelectricity in strained $BaTiO_3$ thin films*, Science **306**, 1005 (2004).

[41] J. H. Haeni, P. Irvin, W. Chang, R.Uecker, P. Reiche, Y. L. Li, S. Choudhury, W. Tian, M. E. Hawley, B. Craigo, A. K. Tagantsev, X. Q. Pan, S. K. Streiffer, L. Q. Chen, S. W. Kirchoefer, J. Levy, and D. G. Schlom, *Room-temperature ferroelectricity in strained $SrTiO_3$*, Nature **430**, 758 (2004).

[42] D. Lebeugle, D. Colson, A. Forget, and M. Viret, *Very large spontaneous electric polarization in $BiFeO_3$ single crystals at room temperature and its evolution under cycling fields*, Appl. Phys. Lett. **91**, 022907 (2007).

[43] J. B. Neaton, C.-L. Hsueh, and K. M. Rabe, *Enhanced polarization in strained $BaTiO_3$ from first principles*, cond-mat/0204511 (2002).

[44] Claudia Bungaro and Karin M. Rabe, *Epitaxially strained [001]-$(PbTiO_3)_1(PbZrO_3)_1$ superlattice and $PbTiO_3$ from first principles*, Phys. Rev. B **69**, 184101 (2004).

[45] Claude Ederer and Nicola A. Spaldin, *Effect of epitaxial strain on the spontaneous polarization of thin film ferroelectrics*, Phys. Rev. Lett. **95**, 257601 (2005).

[46] Claude Ederer and Nicola A. Spaldin, *Influence of strain and oxygen vacancies on the magnetoelectric properties of multiferroic bismuth ferrite*, Phys. Rev. B **71**, 224103 (2005).

[47] Jiefang Li, Junling Wang, M. Wuttig, R. Ramesh, Naigang Wang, B. Ruette, A. P. Pyatakov, A. K. Zvezdin, and D. Viehland, *Dramatically enhanced polarization in (001), (101), and (111) $BiFeO_3$ thin films due to epitaxial-induced transitions*, Appl. Phys. Lett. **84**, 5261 (2004).

[48] Dae Ho Kim, Ho Nyung Lee, Michael D. Biegalski, and Hans M. Christen, *Effect of epitaxial strain on ferroelectric polarization in multiferroic $BiFeO_3$ films*, Appl. Phys. Lett. **92**, 012911 (2008).

[49] Dan Ricinschi, Kwi-Young Yun, and Masanori Okuyama, *A mechanism for the $150\mu C/cm^2$ polarization of $BiFeO_3$ films based on first-principles calculations and new structural data*, J. Phys.: Condens. Matter **18**, L97 (2006).

[50] K. Y. Yun, D. Ricinschi, T. Kanashima, M. Noda, and M. Okuyama, *Giant ferroelectric polarization beyond 150 $\mu C/cm^2$ in $BiFeO_3$ thin films*, Jpn. J. Appl. Phys. **43**, L647 (2004).

[51] Pio Baettig, Claude Ederer, and Nicola A. Spaldin, *First principles study of the multiferroics $BiFeO_3$, Bi_2FeCrO_6, and $BiCrO_3$: Structure, polarization, and magnetic ordering temperature*, Phys. Rev. B **72**, 214105 (2005).

[52] C. Ederer and N. A. Spaldin, *Weak ferromagnetism and magnetoelectric coupling in bismuth ferrite*, Phys. Rev. B **71**, 060401(R) (2005).

[53] I. E. Dzyaloshinskii, *Thermodynamic theory of "weak" ferromagnetism in antiferromagnetic substances*, Sov. Phys. JETP **5**, 1259 (1957).

[54] Wilma Eerenstein, F. D. Morrison, J. Dho, M. G. Blamire, J. F. Scott, and Neil Mathur, *Comment on "Epitaxial $BiFeO_3$ multiferroic thin film heterostructures"*, Science **307**, 1203a (2005).

[55] Feiming Bai, Junling Wang, M. Wuttig, JieFang Li, Naigang Wang, A. P. Pyatakova dn A. K. Zvezdin, L. E. Cross, and D. Viehland, *Destruction of spin cycloid in $(111)_c$-oriented $BiFeO_3$ thin films by epitaxial constraint: Enhanced polarization and release of latent magnetization*, Appl. Phys. Lett. **86**, 032511 (2005).

[56] H. Bea, M. Bibes, S. Petit, J. Kreisel, and A. Barthelemy, *Structural distortion and magnetism of $BiFeO_3$ epitaxial thin films: a Raman spectroscopy and neutron diffraction study*, Philos. Mag. Lett. **87**, 165 (2007).

[57] Yu. F. Popov, A. K. Zvezdin, G. P. Vorob'ev, A. M. Kadomtseva, V. A. Murashev, and D. N. Rakov, *Linear magnetoelectric effect and phase transitions in bismuth ferrite, $BiFeO_3$*, JETP Lett. **57**, 69 (1993).

[58] I. Sosnowska, W. Schäfer, W. Kockelmann, K. H. Andersen, and I. O. Troyanchuk, *Crystal structure and spiral magnetic ordering in $BiFeO_3$ doped with manganese*, Appl. Phys. A **74**, S1040 (2002).

[59] Tôru Moriya, *Anisotropic superexchange interaction and weak ferromagnetism*, Phys. Rev. **120**, 91 (1960).

[60] Claude Ederer and Nicola A. Spaldin, *Electric-field-switchable magnets: The case of $BaNiF_4$*, Phys. Rev. B **74**, 020401(R) (2006).

[61] Craig J. Fennie, *Ferroelectrically induced weak ferromagnetism by design*, Phys. Rev. Lett. **100**, 167203 (2008).

[62] Claude Ederer and Craig J. Fennie, *Electric-field switchable magnetization via the Dzyaloshinskii-Moriya interaction: $FeTiO_3$ versus $BiFeO_3$*, J. Phys.: Condens. Matter **20**, 434219 (2008).

[63] Craig J. Fennie and Karin M. Rabe, *Magnetic and electric phase control in epitaxial $EuTiO_3$ from first principles*, Phys. Rev. Lett. **97** (2006), 267602.

[64] Pio Baettig and Nicola A. Spaldin, *Ab initio prediction of a multiferroic with large polarization and magnetization*, Appl. Phys. Lett. **86**, 012505 (2005).

[65] Riad Nechache, Catalin Haragea, Alain Pignolet, Francois Normandin, Teodor Veres, Louis-Pilippe Carignan, and David Ménard, *Growth, structure, and properties of epitaxial thin films of first-principles predicted multiferroic Bi_2FeCrO_6*, Appl. Phys. Lett. **89**, 102902 (2006).

[66] Matthew R. Suchomel, Chris I. Thomas, Mathieu Allix, Matthew J. Rosseinsky, Andre M. Fogg, and Michael F. Thomas, *High pressure bulk synthesis and characterization of the predicted multiferroic $Bi(Fe_{0.5}Cr_{0.5})O_3$*, Appl. Phys. Lett. **90**, 112909 (2007).

[67] Dae Ho Kim, Ho Nyung Lee, Michael D. Biegalski, and Hans M. Christen, *Large ferroelectric polarization in antiferromagnetic $BiFe_{0.5}Cr_{0.5}O_3$ epitaxial films*, Appl. Phys. Lett. **91**, 042906 (2007).

[68] Alison J. Hatt and Nicola A. Spaldin, *Trilayer superlattices: A route to magnetoelectric multiferroics?*, Appl. Phys. Lett. **90**, 242916 (2007).

[69] Chun-Gang Duan, S. S. Jaswal, and E. Y. Tsymbal, *Predicted magnetoelectric effect in $Fe/BaTiO_3$ multilayers: ferroelectric control of magnetism*, Phys. Rev. Lett. **97**, 047201 (2006).

[70] M. Mostovoy, *Ferroelectricity in spiral magnets*, Phys. Rev. Lett. **96**, 067601 (2006).

[71] H. Katsura, N. Nagaosa, and A. V. Balatsky, *Spin current and magnetoelectric effect in noncollinear magnets*, Phys. Rev. Lett. **95**, 057205 (2005).

[72] I. A. Sergienko and E. Dagotto, *Role of the Dzyaloshinskii-Moriya interaction in multiferroic perovskites*, Phys. Rev. B **73**, 094434 (2006).

[73] I. A. Sergienko, C. Şen, and E. Dagotto, *Ferroelectricity in the magnetic E-phase of orthorhombic perovskites* Phys. Rev. Lett. **97**, 227204 (2006).

[74] S. Picozzi, K. Yamauchi, B. Sanyal, I. A. Sergienko and E. Dagotto, *Dual Nature of Improper Ferroelectricity in a Magnetoelectric Multiferroic*, Phys. Rev. Lett. **99**, 227201 (2007).

[75] H. J. Xiang *et al Spin-Orbit Coupling and Ion Displacements in Multiferroic* $TbMnO_3$, Phys. Rev. Lett. **101**, 037209 (2008).

[76] A. Malashevic and D. Vanderbilt *First Principles Study of Improper Ferroelectricity in* $TbMnO_3$, Phys. Rev. Lett. **101**, 037210 (2008).

[77] H. J. Xiang and M.-H. Whangbo, *Density-Functional Characterization of the Multiferroicity in Spin Spiral Chain Cuprates*, Phys. Rev. Lett. **99**, 257203 (2007).

[78] K. Yamauchi, F. Freimuth, S. Blügel, and S. Picozzi, *Magnetically induced ferroelectricity in orthorhombic manganites: Microscopic origin and chemical trends*, Phys. Rev. B **78**, 014403 (2008).

[79] Hua Wu, T. Burnus, Z. Hu, C. Martin, A. Maignan, J. C. Cezar, A. Tanaka, N. B. Brookes, D. I. Khomskii, and L. H. Tjeng *Ising Magnetism and Ferroelectricity in* Ca_3CoMnO_6, Phys. Rev. Lett. **102**, 026404 (2009).

[80] Y. Zhang, H. J. Xiang, and M.-H. Whangbo *Interplay between Jahn-Teller instability, uniaxial magnetism, and ferroelectricity in* Ca_3CoMnO_6, Phys. Rev. B **79**, 054432 (2009).

[81] C. Wang, G. C. Guo, and L. He, *Ferroelectricity Driven by the Noncentrosymmetric Magnetic Ordering in Multiferroic* $TbMn_2O_5$*: A First-Principles Study*, Phys. Rev. Lett. **99**, 177202 (2007).

[82] G. Giovannetti and J. van den Brink *Electronic Correlations Decimate the Ferroelectric Polarization of Multiferroic* $HoMn_2O_5$, Phys. Rev. Lett. **100**, 227603 (2008).

[83] H. J. Xiang and M.-H. Whangbo *Charge Order and the Origin of Giant Magnetocapacitance in* $LuFe_2O_4$, Phys. Rev. Lett. **98**, 246403 (2007).

[84] M. Alexe, M. Ziese, D. Hesse, P. Esquinazi, K. Yamauchi, T. Fukushima, S. Picozzi, and U. Gösele *Ferroelectric switching in multiferroic magnetite (*Fe_3O_4*) thin films*, unpublished.

[85] G. Giovannetti, S. Kumar, J. van den Brink and S. Picozzi, *Magnetically induced electronic ferroelectricity in half-doped manganites*, arXiv:0812.4380.

[86] G. Giovannetti, S. Kumar, S. Picozzi and J. van den Brink, in preparation.

[87] T. Kimura, *et al. Magnetic control of ferroelectric polarization*, Nature **426**, 55 (2003).

[88] Y. Yamasaki *et al.*, *Electric Control of Spin Helicity in a Magnetic Ferroelectric*, Phys. Rev. Lett. 98, 147204 (2007); Phys. Rev. Lett. 100, 219902(E) (2008).

[89] N. Ikeda, *et al. Ferroelectricity from iron valence ordering in the charge-frustrated* $LuFe_2O_4$, Nature **436**, 1136 (2005).

[90] M. Angst *et al. Charge Order in* $LuFe_2O_4$*: Antiferroelectric Ground State and Coupling to Magnetism*, Phys. Rev. Lett. **101**, 227601 (2008).

[91] G. Kresse and J. Furthmüller, *Efficient iterative schemes for ab initio total-energy calculations using a plane-wave basis set*, Phys. Rev. B **54**, 11169 (1996).

[92] J. P. Perdew, K. Burke, and M. Ernzerhof, *Generalized Gradient Approximation Made Simple*, Phys. Rev. Lett. **77**, 3865 (1996).

[93] E. Wimmer, H. Krakauer, M. Weinert and A. J. Freeman, *Full-potential self-consistent linearized-augmented-plane-wave method for calculating the electronic structure of molecules and surfaces:* O_2 *molecule*, Phys. Rev. B **24**, 864 (1981).

[94] `http://www.flapw.de`

[95] F. Freimuth, Y. Mokrousov, D. Wortmann, S. Heinze, and S. Blügel *Maximally localized Wannier functions within the FLAPW formalism*, Phys. Rev. B **78**, 035120 (2008).

[96] A. Munoz *et al.*, *Complex Magnetism and Magnetic Structures of the Metastable* $HoMnO_3$ *Perovskite*, Inorg. Chem. **40**, 1020 (2001).

[97] J.-S. Zhou, J. B. Goodenough, J. M. Gallardo-Amores, E. Morn, M. A. Alario-Franco, and R. Caudillo *Hexagonal versus perovskite phase of manganite* $RMnO_3$ *(R=Y, Ho, Er, Tm, Yb, Lu)*, Phys. Rev. B **74**, 014422 (2006); J.-S. Zhou and J. B. Goodenough, *Unusual Evolution of the Magnetic Interactions versus Structural Distortions in* $RMnO_3$ *Perovskites*, Phys. Rev. Lett. **96**, 247202 (2006).

[98] M. Tachibana, T. Shimoyama, H. Kawaji, T. Atake, and E. Takayama-Muromachi, *Jahn-Teller distortion and magnetic transitions in perovskite* $RMnO_3$ *(R=Ho, Er, Tm, Yb, and Lu)*, Phys. Rev. B **75**, 144425 (2007).

[99] B. Lorenz, Y. Q. Wang, and C. W. Chu, *Ferroelectricity in perovskite* $HoMnO_3$ *and* $YMnO_3$, Phys. Rev. B **76**, 104405 (2007).

[100] V. Yu. Pomjakushin, M. Kenzelmann, A. Donni, A. B. Harris, T. Nakajima, S. Mitsuda, M. Tachibana, L. Keller, J. Mesot, H. Kitazawa, E. Takayama-Muromachi, *Evidence for large electric polarization from collinear magnetism in* $TmMnO_3$, arXiv:0901.0787.

[101] R. V. Aguilar, *et al.*, *Origin of Electromagnon Excitations in Multiferroic* $RMnO_3$, Phys. Rev. Lett. **102**, 047203 (2009).

[102] G. H. Jonker and J. H. Van Santen, *Ferromagnetic compounds of manganese with perovskite structure*, Physica **16**, 337 (1950).

[103] P. G. Radaelli, D. E. Cox, M. Marezio and S-W. Cheong, *Charge, orbital, and magnetic ordering in* $La_{0.5}Ca_{0.5}MnO_3$, Phys.Rev.B **55**, 3015 (1997).

[104] E. E. Rodriguez, Th. Proffen, A. Llobet, J. J. Rhyne, and J. F. Mitchell, *Neutron diffraction study of average and local structure in* $La_{0.5}Ca_{0.5}MnO_3$, Phys.Rev.B **71**, 104430 (2005).

[105] A. Daoud-Aladine, J. Rodriguez-Carvajal, L. Pinsard-Gaudart, M. T. Fernandez-Diaz, and A. Revcolevschi, *Zener Polaron Ordering in Half-Doped Manganites*, Phys. Rev. Lett. **89**, 097205 (2002).

[106] L. Wu, R. F. Klie, Y. Zhu and Ch. Jooss, *Experimental confirmation of Zener-polaron-type charge and orbital ordering in* $Pr_{1-x}Ca_xMnO_3$, Phys. Rev. B **76**, 174210 (2007).

[107] D. V. Efremov, J. van der Brink, D. I. Khomskii, *Bond- versus site-centred ordering and possible ferroelectricity in manganites*, Nature Materials **3**, 853 (2004).

[108] V. Scagnoli, U. Staub, A. M. Mulders, M. Janousch, G. I. Meijer, G. Hammerl, J. M. Tonnerre, and N. Stojic, *Role of magnetic and orbital ordering at the metal-insulator transition in* $NdNiO_3$, Phys. Rev. B **73**, 100409 (2006).

[109] M. L. Medarde, *Structural, magnetic and electronic properties of* $RNiO_3$ *perovskites (R = rare earth)*, J. Phys.: Condens. Matter **9**, 1679 (1997).

[110] J. A. Alonso, J. L. Garcia-Munoz, M. T. Fernandez-Diaz, M. A. G. Aranda, M. J. Martinez-Lope, and M. T. Casais, *Charge Disproportionation in* $RNiO_3$ *Perovskites: Simultaneous Metal-Insulator and Structural Transition in* $YNiO_3$, Phys. Rev. Lett. **82**, 3891 (1999); J. A. Alonso, M. J. Martinez-Lope, and M. T. Casais, J. L. Garcia-Munoz, M. T. Fernandez-Diaz *Room-temperature monoclinic distortion due to charge disproportionation in* $RNiO_3$ *perovskites with small rare-earth cations (R = Ho, Y, Er, Tm, Yb, and Lu): A neutron diffraction study*, Phys. Rev. B **61**, 1756 (2000).

[111] J. van den Brink J, D.I. Khomskii, *Multiferroicity due to charge ordering*, J. Phys.: Condens. Matter **20**, 434217 (2008).

[112] J. P. Wright *et. al*, *Charge ordered structure of magnetite* Fe_3O_4 *below the Verwey transition*, Phys. Rev. B **66**, 214422 (2002); J. P. Wright, P. Attfield and P. G. Radaelli, *Long Range Charge Ordering in Magnetite Below the Verwey Transition*, Phys. Rev. Lett. **87**, 266401 (2004).

[113] Y. Joly, J. E. Lorenzo, E. Nazarenko, J.-L. Hodeau, D. Mannix, and C. Marin, *Low-temperature structure of magnetite studied using resonant x-ray scattering*, Phys. Rev. B **78**, 134110 (2008).

[114] H.-T. Jeng *et. al*, *Charge-orbital ordering in low-temperature structures of magnetite: GGA+U investigations*, Phys. Rev. B **74**, 195115 (2006).